Response to comments #1

We would like to thank the referee #1 for their constructive and useful comments. This document contains the authors' responses to comments from reviewer #1. Each comment is discussed separately with the following typesetting:

5   *Reviewer's comment

    Author's response

    Changes in the manuscript.

10 *Review for manuscript Comparative assessment of GRASP algorithm for a dust event over Granada (Spain) during ChArMEx-ADRIMED 2013 campaign. Authors provide comparison of inversions of lidar and sun photometers observations using three different algorithms: LIRIC, GARLIC, AERONET operational algorithm, and demonstrate that results are similar. Such comparison is useful, showing that approaches are consistent. On another hand, similarity in results is hardly surprising, because all three algorithms are based on the same 15 principles. Possibility to use two sun photometers at different heights is interesting, because it helps to analyze possible biases due to geometrical overlap effects. I think manuscript can be published after some revision.

General comments:

20 *The main question is what we can conclude from this comparison? Authors write: "Results obtained here show that the combination of lidar and sun photometer data can provide improved and more complete column-integrated data compared to AERONET retrieval." I think this statement is unsupported. The difference between methods is inside the inversion uncertainty. This is just comparison and can not be considered as validation.

25   **The comparison presented here between GRASP versus other algorithms (i.e. AERONET and LIRIC) and with airborne in-situ measurements shows the potential to retrieve aerosol microphysical and optical profiles, and also to obtain fine and coarse mode aerosol refractive index and single scattering albedo which is not possible with the current AERONET inversion. Also, the advance versus LIRIC is that GRASP does not assumes as starting point the results of 30 AERONET inversion.**

*In conclusion they write: "As a future outlook, it will be of great interest to expand the present analysis covering different scenarios including a major variety of aerosol types and loads during campaigns with airborne measurements in order to validate the new improvements". 35 Yes, it is always useful to consider more situations; still it is not validation.

We agree with the referee that the results presents are just an evaluation for two study cases. To perform evaluations of the configuration sun-photometer + lidar signals, we plan to use a synthetic database provided by global models. Initially we will work with GEOS-5 aerosol fields and computing sky radiances using VLDORT radiative transfer code. A complete evaluation using this scheme is in course, but outside the scope of this manuscript.

We add (section 5, page 11, line 19): The analysis presented here is useful as a primary evaluation of the GRASP algorithm using sun-photometer and lidar signal to retrieve aerosol microphysical properties, both integrated along the vertical column and as vertical profiles. The use of a second sun-photometer located over the local atmospheric boundary layer can be very relevant for the study of the properties of aerosol layers with features really different than the atmospheric boundary layer aerosol. However, the presented analysis is representative of Saharan dust transport to south Europe and still it is necessary to use a more complete dataset that includes different aerosol loads and types. In future studies, we could try to use of the combination of one lidar with two sun-sky photometers at different height to try improve the retrievals in the cases with different aerosol layers. In addition, in order to validate the presented GRASP scheme, in the future it is planned to use global aerosol models (e.g. GEOS-5) following an approach similar to Whiteman et al., (2017).

*Expected advantage of combining lidar with sun photometers is ability to profile intensive particle properties, such as effective radius, refractive index, Angstrom exponent. Authors provide profiles of volume and backscattering, so it is difficult to conclude if they observe height dependence of intensive parameters.

The focus of this work was to evaluate GRASP retrieval algorithm against the well-established AERONET inversion retrievals and independent in-situ airborne measurements during Charmex campaign. GRASP is in continuous development and there are intensive parameters profiles that the referee mentions that are not still available and therefore their evaluation is not possible. However, we focused on SSA and Scattering – Angström Exponent, and also other intensive properties such as mean value of backscatter - Angström exponent (β-AE) and Color Ratio (CR).

*Authors write "For 17th June, vertical profiles of SSA are sensitive to the different aerosol layers with different aerosol types illustrating the capabilities of GRASP for detecting different aerosol layers with different composition." But from fig.7, 8 I can conclude in the height range ∼1.8 – 2.7 km backscattering is very low, so variation of SSA in this range is probably just artifact. The same is true for fig.9, variations of AE in this range are probably not real. Do authors have depolarization measurements? Height variation of particle depolarization ratio could provide some information.

We agree with the reviewer that in the mentioned layer the aerosol load is low (~5 μm^3/cm^3 in the range ~1.8 – 2.7 km a.s.l.) and, hence, SSA and AE values could be affected by a large uncertainty. However, the layer below 1.8 km a.s.l. showed a moderate concentration (~17 μm^3/cm^3) and the SSA and AE profiles still reveal a different composition to that of the layer above 2.7 km a.s.l..

We add (section 4.2, page 10, line 21): On 17th June, in the range ~1.8 – 2.7 km a.s.l. the aerosol load was low (~5 µm^3/cm^3) and, hence, SSA and AE values could be affected by larger uncertainties. However, the layer up to 1.8 km a.s.l. showed a moderate concentration (~17 µm^3/cm^3) and the SSA and AE profiles still reveal a different composition with a different composition to that of the layer above 2.7 km a.s.l.

We added the depolarization ratio (δ) quicklook to Figure 2. These figures point out that on 16th June there was a unique layer while on 17th June, there were two main layers: an aerosol layer close to the surface and a decoupled one between 2.7 and 5.5 km a.s.l.. The depolarization ratio evidences that there was an aerosol type below 2.7 km a.s.l. and a different one above this altitude up to 5.5 km a.s.l..

We add (section 4, page 6, line 13): "measurements of δ evidence that there was an aerosol layer below 2.7 km a.s.l. and another aerosol layer above this altitude up to 5.5 km a.s.l.."
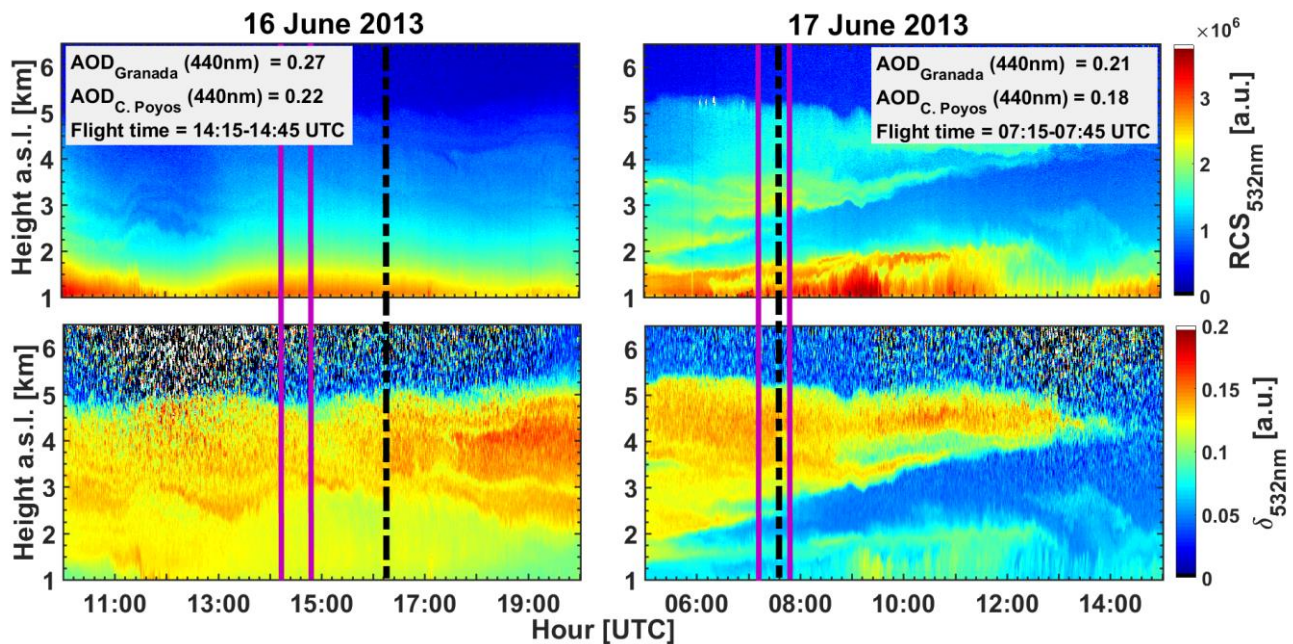

Figure 1. Temporal evolution of the lidar range corrected signal (top) and the depolarization ratio (bottom) at 532nm on 16th (left) and 17th (right) June, 2013. The two purple lines indicate the lidar analyzed interval. The black dashed line indicates the sun-photometer measurements.

Specific comments:

*Fig.3. In Granada imaginary part has spectral dependence typical for dust, while In Cerro Poyos no. Why? PSD look similar. Is it possible to provide vertical profile of imaginary part?

We thank the referee for this comment as we did not notice before. We added the following comment in the manuscript. For the moment, GRASP do not provide vertical profiles of refractive indices.

We add (section 4.1, page 7, line 28): At Cerro Poyos we did not find the spectral dependence of the IRI typically associated to mineral dust. The AOD at 440 nm were around 0.18 - 0.27 and we

used AERONET level 1.5 products, therefore, these values have large uncertainties (> 50%; Dubovik et al., 2000). The lack of spectral dependence can be just an artifact of the inversion. However, it is worthy to note that at Cerro Poyos the PSD shows a mode in the coarse mode size range around 1 μm. As there is still discussion in the scientific community about dust RI and about the differences in dust particles between different sources (e.g. Colarco et al., 2014), results can suggest possible differences in dust RI between long range transported and mixture with local dust injections (the area is very dry in summer, thus favoring local mineral dust resuspension) and local pollution.

*Information about airplane measurements would be useful. Did it ascend by spiral? How much time did it take for one vertical profile?

During the CHARMEX campaign the flights ascended or descended performing a spiral trajectory during 30 min. We have added in Figure 2 the flight time for both days.

We add (section 2.3, page 5, line 1): These flights ascended or descended performing a spiral trajectory during 30 min.

*Fig.6, 17 June, Granada, 355 nm. Why Klett is not given for ~1.8 - 2.5 km? If it is 0, it still should be shown. Why Klett at 355 is not shown below 1.6 km while Grasp retrievals are given? The same questions are for Cerro Poyos.

On 17th June for this range at 355nm the values were 0. We changed the figures and now we show these values.

We add (section 4.2, page 9, line 17): Below 1.6 km, the Klett retrieval at 355 showed unrealistic values probably associated with instrumental problems. However, for GRASP this problem does not appear and seems to be canceled due to the use of the combined data of lidar and sun-photometer.

*References take about 50% of the text volume. Probably too much.

In the revised manuscript, we have reduced the number of references.

Response to comments #2

We would like to thank the referee #2 for their constructive and useful comments. This document contains the authors' responses to comments from reviewer #2. Each comment is discussed separately with the following typesetting:

5   *Reviewer's comment

       Author's response

       Changes in the manuscript.

*General comments: This paper presents the comparative assessment of the GRASP
10 (Generalized Retrieval of Atmosphere and Surface Properties) algorithm aerosol optical properties using combined sunphotometer and lidar measurements with other ground-based lidar products and airborne-based in-situ measurement during ChArMEx-ADRIMED 2013 campaign. The second section of the paper is the explanation of Granada site and instrumentation of ground-based remote sensing (sunphotometer and lidar) and airborne in-
15 situ measurements during the campaign. The list of equipment, retrieved/measured optical properties with algorithm characteristics, and its uncertainties are presented with references. The third section is the explanation of GRASP and LIRIC inversion algorithms. Although both algorithms use the information of combined lidar and sun-sky photometer measurements, the detailed processes are different and described in this section. The main advantage of GRASP
20 is the simultaneous inversion using 180◦ backscattering information of lidar and direct-sun and almucantar measurement of sky radiance by sun-sky radiometer. The fourth section contains the comparison results of GRASP and other measurements according to different optical properties: column-integrated properties such as size distribution, effective radii of course and fine modes, volume concentration, refractive indices, and single scattering
25 albedo, and vertically-resolved properties such as volume concentration, extinction and backscatter coefficient profiles, single scattering albedo, and scattering Ångström Exponent. Most aerosol optical properties of GRASP show similar results with other measurements, but also provide different information such as coarse mode shift to higher radii compared to AERONET-only or more information such as profiles of SSA and scattering Ångström
30 Exponent compared to LIRIC.

The paper presents an abundant comparison results of GRASP with other measurement during the campaign, and the results are clear. The scope is well-addressed also, thus I recommend it for publication after the responses for some points listed hereafter.

35

Specific comments/questions:

*In section 2.1, the distribution of observation sites or geological map could help to understand geographical conditions although the located information is described in manuscript because the authors explain apparent errors as the different location of measurement sites at some compared aerosol optical properties.

We agree with the referee and we have added a map illustrating the Granada and Cerro Poyos stations.

We add in the manuscript (section 2.1, page 3, line 21): Figure 1 shows a map illustrating the distance between Granada and Cerro Poyos stations.

We add in the manuscript (section 2.3, page 5, line 2): Figure 1 shows the spiral trajectory of F31 flight that is similar to that of F30, covering in both cases the same atmospheric column.
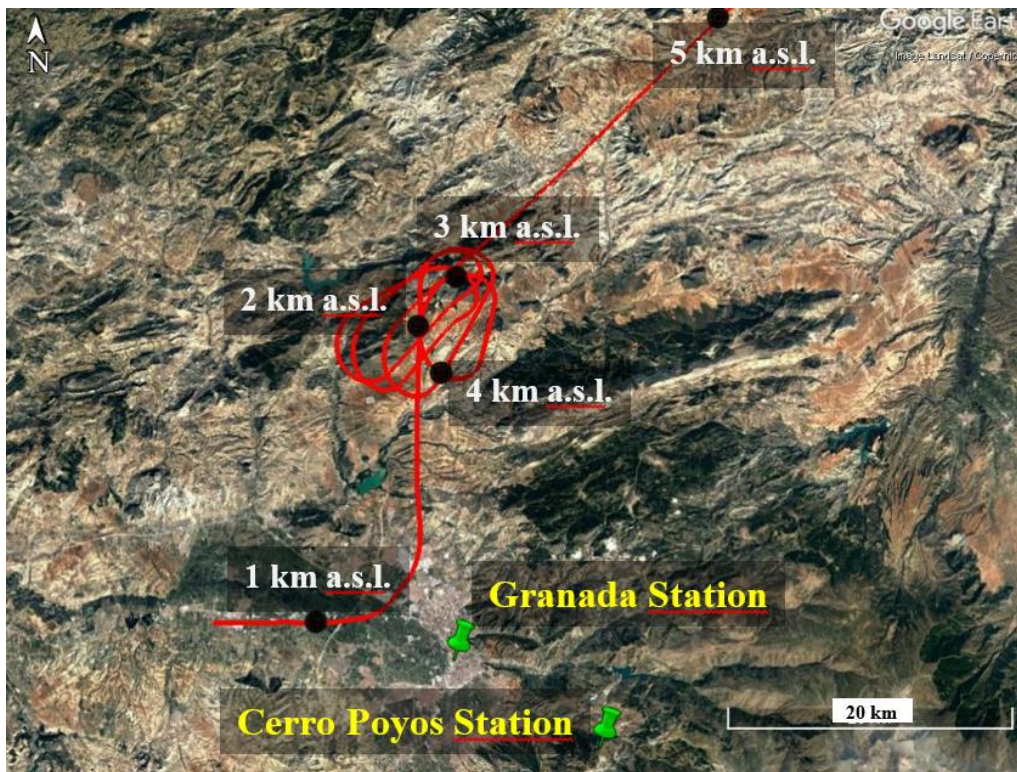

Figure 2. Map illustrating the Granada and Cerro Poyos stations. The red line indicates the trajectory and the black points the altitude of the aircraft on 17th June

*In section 2.2 (page 4 line 16), recent AERONET data version is changed from 2 to 3. Although the version of inversion data is still version 2, please notate the data version (i.e. version 2).

We added the AERONET data version used in this paper (version 2).

6

We changed (section 2.2, page 4, line 17): "In this work, the AERONET Version 2 Level 2.0 data obtained at Granada and Cerro Poyos during ChArMEx-ADRIMED 2013 are used."

* In section 3, please describe the input and output information of lidar and sunphotometer for LIRIC and GRASP specifically (i.e. which wavelength of sky-radiance of sunphotometer, lidar measurement as input, and which column-integrated/vertical aerosol optical properties as output).

We add a new table with input/output information used/retrieved by GRASP and LIRIC.

We add the following sentence (section 3, page 5, line 21): "The input information needed by GRASP and LIRIC algorithms and the aerosol properties retrieved and used in this work are shown in Table 2".

Table 2. Input and output information used for LIRIC and GRASP retrievals.

	LIRIC		GRASP	
	SUN-PHOTOMETER*	LIDAR	SUN-PHOTOMETER	LIDAR
INPUT	• AOD • VC • RRI and IRI • % Sphericity	Elastic backscattered signal: • 355, 532 and 1064 nm • 532-cross polarized signal	• AOT or AOD • Total scattered radiances At 440, 670, 870 and 1020 nm	Elastic backscattered signal: • 355, 532 and 1064 nm
OUTPUT	• VC profile for fine and coarse mode		Columnar (fine and coarse) • SD • RRI and IRI • VC • r_{eff} • SSA • LR • % Sphericity (total)	Vertical (fine and coarse) • VC • α and β • SSA

*AERONET product

*In section 3 (page 5 line 31), Which information of the photometer is provided for lidar retrievals? Please describe "otherwise" (the assumption in lidar measurements) more specifically.

The sun-photometer provides the aerosol optical depth and the combination of direct sun and sky radiances provides column-integrated aerosol microphysical properties. Sun-photometer measurements, collocated with backscatter lidar, are used to estimate extinction-to-backscatter ratio, typically known as lidar ratio (LR). If there are no collocated sun photometer, the LR assumption are based on climatological values.

We changed (section 3, page 5, line 35): "… and the photometer data provides the information (e.g. amount and type) required for lidar retrievals that otherwise would be assumed from climatological data (Bovchaliuk et al., 2016)"

*In section 4 (figure 1), what is the definition of the lidar range corrected signal? Is it calculated as P*r2, where P is the lidar data (received power) and r is the range?

Yes, the referee is right.

We add the following sentence (section 4, page 6, line 9): The RCS is calculated as P*r2, where P is the lidar signal (corrected from background and dark current) and r is the altitude.

*In section 4.1 (page 7 line 11 and 27): the authors mentioned that the wavelength of RRI and IRI from airborne measurement is 500 nm. However, it is not on the 500 nm in the Figure 3. Please clarify it.

We made a mistake in the text but not in figure 3. The wavelength of RRI and IRI from airborne measurements is 530 nm and not 500 nm. We have changed it in section 4.1.

*In section 4.1, which height is represented from the airborne measurement? Would it be possible reason of difference because lidar profile shows different concentration in 17 June?

We think that the referee refers to section 4.2 indeed, where we use airborne data. Height is above sea level (a.s.l.) which is the same than for lidar data.

We believe that the differences in particle volume concentrations between GRASP and airborne data below 2km a.s.l on 17th June are explained because the flight was not exactly over Granada city as shown in Fig. 1 and in the firsts kilometers of the atmosphere could be more differences in the horizontal.

We add (section 4.2, page 9, line 4): On 17th June for Granada retrieval, the differences between both algorithms and airborne data below 2 km a.s.l. could be explained because the flight was not exactly over Granada city as shown in Fig. 1 and in the first two kilometers of the atmosphere differences are expected because of the influence of the city.

*In section 4.1 (page 7 line 32) which wavelength for SSA of "0.80-0.90"?

Thanks to the referee comments we notice that there was a misspelling in the current version of the manuscript.

We changed this sentence in the text (section 4.1, page 8, line 14): "The retrieved SSA values are in the range between 0.85-0.98 (355-1064 nm wavelength range) and are in the ranges…"

*In section 4.2 (page 8 line 30), please briefly describe difference in the method of "Klett" and "GRASP" in terms of lidar ratio (LR).

The Klett uses the assumption of constant LR for the entire column. LR ratio were computed fitting the integral of the extinction to the measured aerosol optical depth. However, GRASP retrieves the LR (fine and coarse) directly from the sun-photometer and lidar measurements. The text has been modified in the methodology section to clarify these points.

We add (section 4.2, page 9, line 12): The LR used in Klett method is assumed constant for the entire profile and was computed by fitting the integral of the different extinction profiles to the measured aerosol optical depth. However, GRASP uses both sun/sky radiances and the backscatter lidar data to provide LR values, both in column-integrated and vertical profiles.

*In section 4.2, (page 8 line 39), could you explain why the discrepancies b/w two B-coeffi products are getting larger in longer wavelength although the error range of GRASP B-coeffi profile is smaller in longer wavelength in Granada on 16th June and Cerro Poyos on 17th June?

Only two study cases are presented here, so we cannot assume that discrepancies are larger for longer wavelengths or that the error range is smaller for a certain wavelength. An additional study, with a synthetic database provided by global models and an analysis with more cases, would be needed to get to significant conclusions in this respect. In the cases presented here, the discrepancies between the backscatter coefficient retrieved by Klett and GRASP were within the uncertainties for our system (~30%).

*In section 4.3 (page 9 line 12), could you show the error range of SSA profiles from GRASP? It could be useful information to understand this SSA profiles because the AODs of all cases are less than 0.3 and SSA error could be large.

GRASP developers are currently doing in depth studies of errors in SSA, and therefore, we are not able to provide them. That was commented in section 3.

*In section 5 (page 10 line 20), I agree for the combination of lidar and sun-photometer data in GRASP algorithm can provide improved and more complete data compared to AERONET retrieval. The refractive indices of GRASP show better agreement with in-situ measurement compared to those of AERONET. However, the column integrated size distribution and SSA doesn't show any in-situ measurement results together. Could you quantify the improvement in GRASP compared to AERONET measurement?

We cannot compare the column-integrated size distribution between GRASP, AERONET and in-situ measurements because the latter are not available. For to quantify the improvement of GRASP compared to AERONET would be necessary study more cases with more in-situ measurements at different wavelengths. However, we add the column-integrated SSA value measured in-situ in Figure 5.

We modified the text (section 4.1, page 8, line 8): Moreover, the SSA value at 530 nm calculated by Denjean et al. (2016) for dust layer using airborne measurements during the campaign was 0.95 ±0.04. SSA retrieved by GRASP at 532 nm are close to the airborne value. Better agreement with this value is found for the retrievals from Granada on 16th June and at Cerro Poyos on 17th June. The differences from Granada on 17th June could be due the in-situ value was calculated for the dust layer whereas that GRASP and AERONET use sun-photometer data, which measures the total atmospheric column. Furthermore, in the case of Granada station, these measures could be influenced by injections of local pollution.
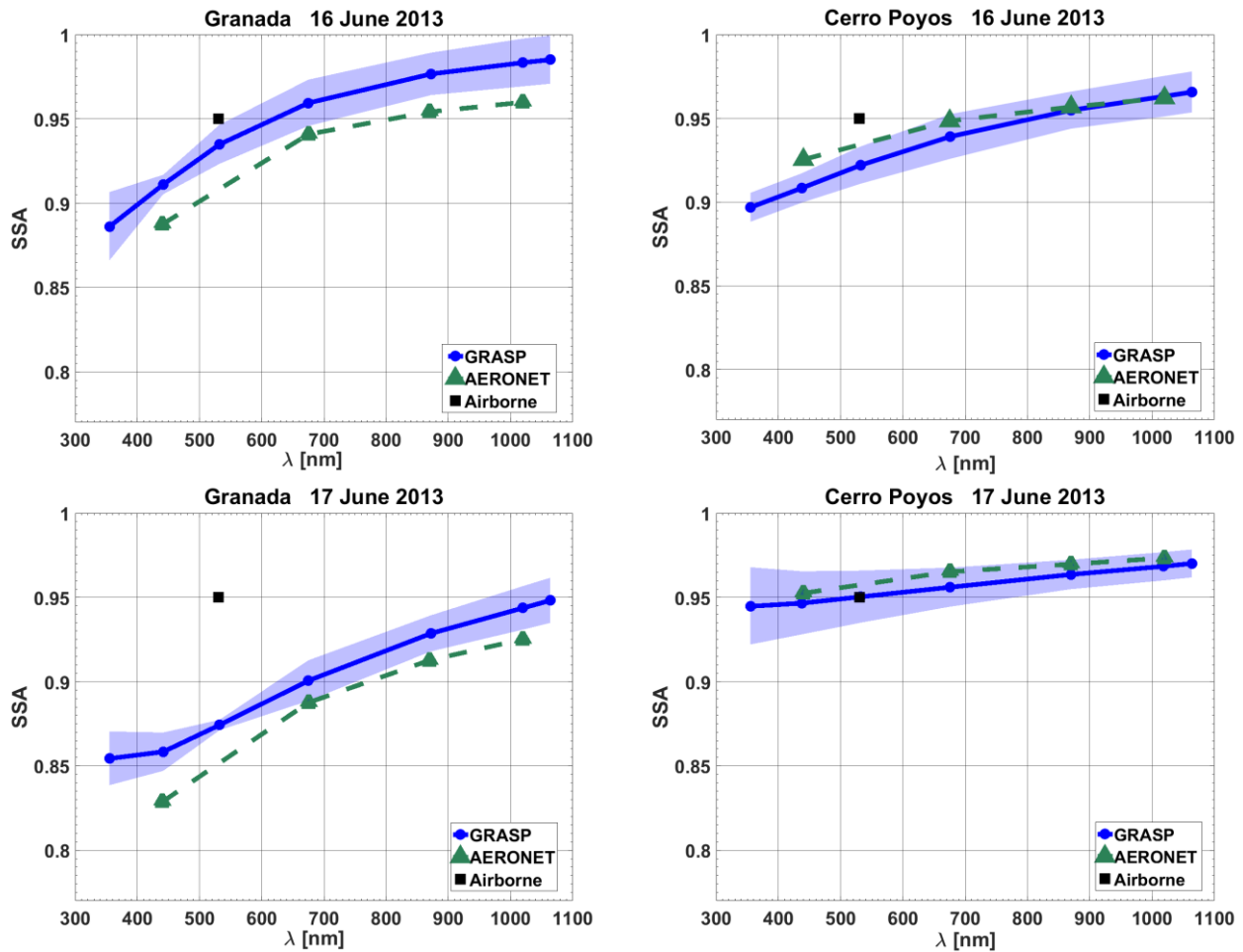

Figure 5. Single-scattering albedo retrieved by GRASP (blue) with its uncertainty (shaded area), AERONET (green) and airborne measurement (black) on 16th (top) and 17th (bottom) June 2013 at Granada (left) and Cerro Poyos (right).

* In Section 5 (page 10 line 29-30), please explain which the improvements of GRASP are new and the method of a second sun-sky photometer in your plan. Is the three instruments combination as one lidar and two sun-photometers in GRASP?

GRASP exploits the synergy among lidar and sun-photometer data just providing enhanced column integrated retrievals over the standard AERONET approach and at the same time allows a profiling of some aerosol microphysical properties. The use of a second sun-photometer located over the local atmospheric boundary layer can be very relevant for the study

of the properties of aerosol layers with features really different than the atmospheric boundary layer aerosol. Thus, the use of the second photometer can be crucial for monitoring microphysics of long range transported particles in the free troposphere. In response to referee question: Yes, in the future, we could try to use of the combination of one lidar with two sun-sky photometers
5 **at different height.**

We decided delete this sentence and we add the following conclusion:

We add (section 5, page 11, line 19): The analysis presented here is useful as a primary evaluation of the GRASP algorithm using sun-photometer and lidar signal to retrieve aerosol microphysical properties, both integrated along the vertical column and as vertical profiles. The use of
10 a second sun-photometer located over the local atmospheric boundary layer can be very relevant for the study of the properties of aerosol layers with features really different than the atmospheric boundary layer aerosol. However, the presented analysis is representative of Saharan dust transport to south Europe and still it is necessary to use a more complete dataset that includes different aerosol loads and types. In future studies, we could try to use of the combination of one lidar with two sun-sky
15 photometers at different height to try improve the retrievals in the cases with different aerosol layers. In addition, in order to validate the presented GRASP scheme, in the future it is planned to use global aerosol models (e.g. GEOS-5) following an approach similar to Whiteman et al., (2017).

Technical correction:

20 Please check whether the typos I found are correct.

*In section 2.1 (page 3 line 31) it local sources → its local sources

We have changed "it local sources" by "its local sources" as suggested.

*In section 2.2 (page 4 line 20), removing ")".

We have removed ")" as suggested.

25 *In section 3 (page 5 line 29): lidar "an" sun-sky photometer measurements → lidar "and" sun-sky.

We have changed "lidar 'an' sun-sky photometer measurements" by "lidar 'and' sun-sky" as suggested.

*In section 3 (page 5 line 35), please write full name of "CRI" (is it "components of refractive
30 indices"?)

CRI is Complex Refractive Indices. Due to that CRI is used only one time in the paper we decided changed it by "RRI, IRI" (real and imaginary refractive indices).

*In section 5 (page 10 line 29), vaity → variety

This word does not appear now.

Response to comments #3

We would like to thank to the editor Dr. Dulac for their constructive and useful comments. This document contains the authors' responses to comments from the editor. Each comment is discussed separately with the following typesetting:

5 *Reviewer's comment

Author's response

Changes in the manuscript.

*I encourage a revision that carefully addresses reviewers comments, especially the strong
10 criticisms raised by referee #1.

Technical corrections:

*In the conclusion, specifiy "complete lidar overlap range" in the begining of line 4

We add (section 5, page 10, line 31): Data from a second photometer at 1.2 km above the lidar system are also used, in this way avoid problems due to incomplete overlap.

15

*Check uodated reference for Torres et al. paper submitted to ACP, which is now in press;

The reference for Torres et. al. (2016) submitted to AMT is what we have in the manuscript. We changed this reference by the following:

Torres, B., Dubovik, O., Fuertes, D., Schuster, G., Cachorro, V. E., Lapionak, T., Goloub, P.,
20 Blarel, L., Barreto, A., Mallet, M., Toledano, C., and Tanré, D.: Advanced characterization of aerosol properties from measurements of spectral optical depth using the GRASP algorithm, Atmos. Meas. Tech., Accepted. 2017.

*Please use larger characters and bold style in order to improve the readability of axes
25 legends and box legends in figures 2-4.

We improved the readability of the figures and modified them in the revised manuscript.

Comparative assessment of GRASP algorithm for a dust event over Granada (Spain) during ChArMEx-ADRIMED 2013 campaign.

J. A. Benavent-Oltra[1,2], R. Román[1,2], M. J. Granados-Muñoz[1,2], D. Pérez-Ramírez[1,2], P. Ortiz-Amezcua[1,2], C. Denjean[3], A. Lopatin[4], H. Lyamani[1,2], B. Torres[4,5], J. L. Guerrero-Rascado[1,2], D. Fuertes[5], O. Dubovik[4], A. Chaikovsky[6], F. J. Olmo[1,2], M. Mallet[3], and L. Alados-Arboledas[1,2]

[1]Department of Applied Physics, University of Granada. 18071, Granada, Spain.
[2]Andalusian Institute for Earth System Research (IISTA-CEAMA), University of Granada, Autonomous Government of Andalusia. 18006, Granada, Spain.
[3]CNRM, Centre National de la Recherche Météorologique (UMR3589, CNRS, Météo-France), Toulouse, France.
[4]Laboratoire d'Optique Atmosphérique, Université de Lille 1, Villeneuve d'Ascq, France.
[5]GRASP-SAS, Remote sensing developments, LOA / Université Lille -1, Villeneuve d'Ascq, France.
[6]Institute of Physics, National Academy of Science, Minsk, Belarus.

Correspondence to: Jose Antonio Benavent-Oltra (jbenavent@ugr.es)

Abstract. In this study, vertical profiles and column-integrated aerosol properties retrieved by GRASP (Generalized Retrieval of Atmosphere and Surface Properties) algorithm are evaluated with in-situ airborne measurements made during the ChArMEx-ADRIMED field campaign in summer 2013. In the framework of this campaign, two different flights took place over Granada (Spain) during a desert dust episode on 16th and 17th June. GRASP algorithm combining lidar and sun-sky photometer data measured at Granada, has been used for retrieving aerosol properties. Two sun-photometers datasets are used: one co-located with the lidar system and a second one in the Cerro Poyos station, approximately 1200 m higher than the lidar system, but at a short horizontal distance.

Column-integrated aerosol microphysical properties retrieved by GRASP are compared with AERONET products showing a good agreement. Differences between GRASP retrievals and airborne extinction profiles are in the range 15% to 30%, depending on the instrument onboard the aircraft used as reference. On 16th June, a case where the dust layer was coupled to the aerosol layer close to surface, the total volume concentration differences between in-situ data and GRASP retrieval are 15% and 36% for Granada and Cerro Poyos retrievals, respectively. On the other hand, on 17th June the dust layer was decoupled from the aerosol layer close to surface, the differences are around 17% for both retrievals. In general, all the discrepancies found are within the uncertainly limits, showing the robustness and reliability of GRASP algorithm. However, the better agreement found for Cerro Poyos retrieval with the aircraft data and the vertical homogeneity of certain properties retrieved with GRASP, such as the scattering - Angström Exponent, for cases with aerosol layers characterized by different aerosol types show that uncertainties in the vertical distribution of the aerosol properties have to be considered.

1 Introduction

Atmospheric aerosols play an important role in the Earth-Atmosphere radiative system due to their interaction with solar and terrestrial radiation and to their role in clouds development and precipitation (Boucher et al., 2013). Uncertainties associated with the interaction of atmospheric aerosols with radiation have been reduced in the last years, but there is still a need for improvements mainly in those aspects related to their absorption properties (IPCC, 2013). The characterization of aerosol vertical distribution is another point of interest to reduce uncertainties associated with atmospheric aerosol particles, since they can be different near the surface, within the boundary layer, and in the free troposphere.

Passive remote sensing offers large advances in aerosol characterization with global sun-photometry networks such as the Aerosol Robotic Network (AERONET; Holben et al., 1998) or lunar/star photometry measurements (Pérez-Ramírez et al.,

2012; Barreto et al., 2016, 2017). In the last years, different inversion methods, based on spectral aerosol optical depth measurements (AOD), were developed for the retrieval of aerosol microphysical properties such as effective radius (r_{eff}) and volume concentration (VC) (e.g. Pérez-Ramírez et al., 2015; Torres et al., 2017). Furthermore, other sophisticated algorithms, that use also sky-radiance measurements, were developed for the retrieval of aerosol microphysical properties as well as intensive properties such as single scattering albedo (SSA), asymmetry parameter and aerosol refractive index (RI) (e.g. Nakajima et al., 1996; Dubovik and King, 2000; Olmo et al., 2006, 2008). Nevertheless, all these algorithms/measurements only provide column-integrated aerosol properties.

Since the 70s, lidar systems are being widely used to characterize aerosol vertical distributions in order to contribute to reduce the radiative forcing uncertainties associated to the atmospheric aerosol. The most basic systems use only information of elastic lidar signal to derive backscatter coefficient by aerosol particles, but require assumption about the extinction-to-backscatter ratio (lidar ratio, LR) (Fernald et al., 1972; Klett, 1981; Fernald, 1984; Klett, 1985). More advance systems such as Raman (Ansmann et al., 1992; Whiteman et al., 1992) and HSRL (High Spectral Resolution Lidar) (Shipley et al., 1983; Grund and Eloranta, 1991) are able to provide independent measurements of backscatter and extinction coefficients (β and α, respectively) without LR assumption. Also, the depolarization measurements are a lidar improvement that provide information about shape of aerosols and allows to characterize the aerosol type (Murayama et al., 2004; Miffre et al., 2011; Bravo-Aranda et al., 2013). However, lidar observations dedicated to the aerosol characterization are very scarce compared to the sun-photometer measurements, and many international networks have emerged in the last decades to homogenize and explore such information. This is the case of the global NASA MPLNET network (Micro-Pulse Lidar Network; Lewis et al., 2016) developed for continuous measurements of aerosol and cloud vertical profiles at different sites in the world using standard instrument and data processing algorithms. The EARLINET (European Aerosol Research LIdar NETwork) (Pappalardo et al., 2014) and LALINET networks (Latin American Lidar Network) (Guerrero-Rascado et al., 2016) have also been established in order to provide long term database for the vertical and temporal distribution of aerosols over Europe and Latin America, respectively.

The retrieval of particle vertical microphysical properties from multiwavelength lidar systems is possible by inverting measurements of three aerosol backscatter and two extinction coefficients, known as the $3\beta+2\alpha$ configuration, using the algorithms developed by Müller et al. (1999), Böckmann (2001) and Veselovskii et al. (2002). However, $3\beta+2\alpha$ measurements are scarce compared with the large database of elastic lidar measurements. In this sense, different inversion methods were recently developed within the framework of EARLINET in order to retrieve vertical profiles of aerosol microphysical properties using combined information of elastic lidar and sun-photometry measurements. Such kind of approaches were the LIdar-Radiometer Inversion Code (LIRIC; Chaikovsky et al., 2008, 2012, 2016) that provides vertical distribution of volume concentrations, and the Generalized Aerosol Retrieval from Radiometer and LIDAR Combined data (GARRLiC; Lopatin et al., 2013) that also allows the retrieval of SSA and RI. Currently, GARRLiC algorithm is included in the Generalized Retrieval of Atmosphere and Surface Properties inversion code (GRASP; Dubovik et al., 2011). However, very few studies have attempted to evaluate this recently developed inversion algorithm (Lopatin et al., 2013; Bovchaliuk et al., 2016; Torres et al., 2017; Román et al., 2017), and therefore their evaluation under different atmospheric conditions is still necessary.

Field campaigns with state of the art instrumentation offer unique possibilities for the evaluation of new retrievals techniques of particle microphysical and optical properties. Recently, the ADRIMED (Aerosol Direct Radiative Impact on the regional climate in the MEDiterranean region) field campaign, which was part of the international cooperative research program Chemistry-Aerosol Mediterranean Experiment (ChArMEx; Dulac et al., 2014), was carried out with the main

objective of capturing the high complexity of the different aerosol types in the Mediterranean region (Mallet et al., 2016). Several in-situ and remote sensing measurements both from surface and on airborne platforms were collected during this campaign using state of the art instrumentation. The measurements were performed at different stations over the western Mediterranean region during summer 2013, to gather an updated database of the physical, chemical and optical aerosol properties as well as the vertical distribution of the major "Mediterranean aerosols" (Mallet et al., 2016; Denjean et al., 2016). Data gathered during ChArMEx-ADRIMED campaign give us an excellent opportunity to evaluate the recently developed algorithms for retrieving aerosol microphysical and optical profiles.

In that framework, the main objective of this study is to evaluate the aerosol optical and microphysical properties obtained with GRASP during the ChArMEx-ADRIMED field campaign in Granada, Spain. The GRASP configuration evaluated in this study here is the one that combines lidar signals and sun-sky radiance measurements. The paper is structured as follows: Section 2 gives a brief description of the experimental site and the instrumentation employed in this study. GRASP and LIRIC codes are described in detail in Section 3. The results are discussed in Section 4 and, finally, the main conclusions are summarized in Section 5.

2 Site and Instrumentation

2.1 Experimental site

The experimental measurements were obtained over Granada region (Spain) at the Andalusian Institute for Earth System Research (IISTA-CEAMA) of the University of Granada, Spain (37.16º N, 3.61º W, 680 m a.s.l.) and at remote high mountain site Cerro Poyos (37.11º N, 3.49º W, 1820 m a.s.l.), located at Sierra Nevada mountain range about 12 km away (horizontally) from IISTA-CEAMA station. **Figure 1 shows a map illustrating the distance between Granada and Cerro Poyos stations.** The city of Granada is located in south-eastern Iberian Peninsula, and is a non-industrialized medium-sized city with a population around 300,000 (twice including the metropolitan area). The city is sited in a natural basin surrounded by mountains with elevations between 1000 and 3500 m a.s.l.. The area is approximately 200 km from the African continent and approximately 50 km from the western Mediterranean basin. In Granada, one main source of natural aerosol is the long-range transport of mineral dust particles from North Africa (e.g. Lyamani et al., 2005; Valenzuela et al., 2012a) that reaches the area in lofted layers (Müller et al., 2009; Guerrero-Rascado et al., 2008, 2009; Córdoba-Jabonero et al., 2011) before mixing with the atmospheric boundary layer (Bravo-Aranda et al., 2015) and been detected at the surface tor in precipitation samples (Calvo et al., 2010). Another natural source is biomass burning particles: fresh smoke (Alados-Arboledas et al., 2011) and long-range transported smoke (Ortiz-Amezcua et. al., 2014, 2017). While the main anthropogenic sources are pollution from Europe, the Iberian Peninsula and the Mediterranean Sea (Lyamani et al., 2006, Pérez-Ramírez et al., 2016), **its local sources** are mainly road traffic and central heating systems (Lyamani et al., 2012; Titos et al., 2017).

2.2 Ground-based instrumentation

Columnar aerosol properties during daytime were obtained by CIMEL CE-318-4 (*Cimel Electronique*) sun-sky photometers at IISTA-CEAMA and Cerro Poyos sites. The sun-photometer instruments used in this study are operated in the framework of AERONET - RIMA network (Iberian Network for Aerosol Measurements, federated to AERONET) (https://aeronet.gsfc.nasa.gov/). A complete description of the instrument can be found in Holben et al. (1998). Briefly, this instrument makes direct solar irradiance measurements at 340, 380, 440, 670, 870 and 1020 nm and sky radiance

measurements at 440, 670, 870 and 1020 nm. Solar direct irradiance measurements are used to calculate the AOD at 340, 380, 440, 670, 870 and 1020 nm, with uncertainty of ±0.01 for $\lambda > 400$ nm and of ±0.02 for $\lambda < 400$ nm (Holben et al., 1998; Eck et al., 1999). Furthermore, the Angström Exponent (AE), parameter that describes the spectral dependency of the AOD, is calculated in the range 440–870 nm. AE provides an indication of the particle size: small values (< 0.5) suggest a predominance of coarse particles, while large values (> 1.5) indicate a predominance of small particles (e.g., Dubovik et al., 2002). The solar direct irradiance and sky radiance measurements are used to retrieve aerosol optical and microphysical properties such as columnar particle size distribution (PSD), real and imaginary refractive indices (RRI and IRI) and SSA, using the algorithm of Dubovik et al. (2006). In addition, the inversion code provides other variables such as the VC, r_{eff} and standard deviation for fine and coarse modes of the retrieved PSD. The uncertainty of the AERONET inversion products is described by Dubovik et al. (2000). Briefly, the uncertainty in the retrieval of SSA is ±0.03 for high aerosol load ($AOD_{440} > 0.4$) and solar zenith angle $> 50º$. For measurements with low aerosol load ($AOD_{440} < 0.2$), the retrieval accuracy of SSA (λ) drops down to 0.02–0.07 (Dubovik et al., 2000). For high aerosol load and solar zenith angle $> 50°$, errors are about 30%–50% for the imaginary part of the RI. For particles in the size range $0.1 < r < 7$ μm, errors in PSD retrievals are around 10–35%, while for sizes lower than 1 μm and higher than 7 μm retrieval errors rise up to 80–100%.

In this work, the AERONET Version 2 Level 2.0 data obtained at Granada and Cerro Poyos during ChArMEx-ADRIMED 2013 are used. However, due to the strong limitations imposed by the AERONET inversion algorithm ($AOD_{440} > 0.4$ and solar zenith angle $> 50°$) there was no SSA and RI AERONET level 2.0 retrievals during the campaign. Thus, for comparing AERONET SSA values with GRASP retrievals, the AERONET level 1.5 cloud screened data corresponding to $AOD > 0.2$ and solar zenith angle $> 50°$ are used in this study.

The multi-wavelength Raman lidar MULHACEN, based on a customized version of LR331D400 (Raymetrics S.A.), is used for obtaining vertical profiles of the atmospheric aerosol properties. This system located at Granada, was incorporated to EARLINET in April 2005, being at present a contributing station to ACTRIS research infrastructure (Aerosols, Clouds, and Trace gases Research InfraStructure Network) (http://actris2.nilu.no/). The system has a monostatic biaxial configuration alignment, pointing vertically to the zenith and uses a pulsed Nd:YAG laser with 2nd- and 3rd-harmonic generators, that emits simultaneously pulses at 1064, 532 and 355 nm. The receiving system consists of several detectors, which can split the radiation according to the three elastic channels at 355, 532 (parallel- and perpendicular-polarized; Bravo-Aranda et al., 2013), and at 1064 nm; two nitrogen Raman channels at 387 and 607 nm (shifted signal from radiation at 355 and 532 nm, respectively); and a water vapor Raman channel at 408 nm (shifted signal from radiation at 355 nm; Navas-Guzmán et al., 2014). More information can be found in Guerrero-Rascado et al. (2008). The aerosol particle backscatter coefficient profiles obtained from the multi-wavelength lidar were obtained by the Klett-Fernald method (Fernald et al., 1972; Klett, 1981; Fernald, 1984; Klett, 1985). Total uncertainty in the profiles obtained with Klett method is usually 20% for β and 25-30% for α profiles (Franke et al., 2001; Preißler et al., 2011). The procedure suggested by Wandinger and Ansmann (2002) was applied to the lidar data to correct the incomplete overlap. Without correction, the complete overlap for this instrument is above 1200 m a.g.l. (Navas-Guzmán et al., 2011).

2.3 Airborne measurements

During the period from 14th June to 4th July 2013, 16 flights were performed in the framework of ChArMEx-ADRIMED over the Mediterranean Basin with the ATR-42 aircraft of SAFIRE (French aircraft service for environmental research; http://www.safire.fr). **These flights ascended or descended performing a spiral trajectory during 30 min.** Two of these flights (flight number F30 and F31) took place over Granada on 16th and 17th June 2013, respectively. **Figure 1 shows the**

spiral trajectory of F31 flight that is similar to that of F30, covering in both cases the same atmospheric column. Flight details are described by Mallet et al. (2016) and Denjean et al. (2016).

Table 1 summarizes the instrumentation onboard the ATR-42 airplane used in this study. The Scanning Mobility Particle Sizer (SMPS) with an accuracy of 5% (Wiedensohler et al., 2012) and the Ultra-High Sensitivity Aerosol Spectrometer (UHSAS) with an accuracy of 10% (Cai et al., 2008) are used for measuring aerosol number size distribution in the submicron range. The wing-mounted Forward Scattering Spectrometer Probe, model 300 (FSSP-300) with an accuracy of 30% (Baumgardner et al., 1992) and the in-cabin GRIMM OPC (sky-OPC 1.129) with an accuracy of 10% (Denjean et al., 2016) were used to measure the optical size distributions in the diameter nominal size range between 0.28 and 20 µm and between 0.3 and 32 µm, respectively. The total particle volume concentrations in the diameter range 0.1-30 µm and volume concentrations of fine (0.1-1 µm) and coarse (1-30 µm) modes were calculated from the measured aerosol number size distributions, assuming that aerosol particles are spherical.

In addition, the nephelometer TSI (model 3563) was used to measure particle scattering coefficients at three wavelengths (450, 550 and 700nm) with an accuracy of 5% (Müller et al., 2011) and a Cavity Attenuated Phase Shift (CAPS) was employed to obtain particle extinction coefficient at 530 nm with an accuracy of 3% (Massoli et al., 2010). Also, the PLASMA (Photomètre Léger Aéroporté pour la Surveillance des Masses d'Air) system, which is an airborne sun-tracking photometer, was used to obtain AOD with wide spectral coverage (15 channels between 0.34 – 2.25 µm) with an accuracy of approximately 0.01 (Karol et al., 2013), as well as the particle extinction vertical profiles (Torres et al., 2017).

3 GRASP and LIRIC inversion algorithms

The input information needed by GRASP and LIRIC algorithms and the aerosol properties retrieved and used in this work are shown in Table 2. LIRIC algorithm provides height-resolved aerosol volume concentration data for the fine and coarse modes from combined lidar **and** sun-sky photometer information (Chaikovsky et al., 2008, 2012; Granados-Muñoz et al., 2014; Chaikovsky et al., 2016). For this, column-integrated aerosol properties provided by the AERONET code (Dubovik et al., 2002, 2006) are used as input, together with the lidar elastic backscatter signals at three different wavelengths (355, 532, and 1064 nm). These data are put through an iterative procedure based on the Levenberg–Marquardt method, which is described in detail in Chaikovsky et al. (2016). Besides the volume concentration, the algorithm retrieves additional data sets, including profiles of particle α and β coefficients, and LR among others. AERONET column-integrated products used as input are not modified by LIRIC during the retrieval process.

The GRASP inversion code (Dubovik et al., 2011; Lopatin et al., 2013), was developed at Laboratoire d'Optique Atmospherique (LOA) of the University of Lille. GRASP is based on a similar philosophy than LIRIC code, but goes a step further since it simultaneously inverts both the coincident lidar and sun-sky photometer measurement, retrieving vertical, but also column, aerosol optical and microphysical properties for both fine and coarse modes. The simultaneous inversion of lidar and sun-sky photometer measurements is expected to improve the retrievals since the lidar data complement the sky photometer measurement at scattering angles of 180º **and the photometer data provides the information (e.g. amount and type) required for lidar retrievals that otherwise would be assumed from climatological data (Bovchaliuk et al., 2016).** Therefore, the column aerosol properties obtained by GRASP will differ from the AERONET ones. Additionally, it is worth to note that GRASP allows independently retrieving aerosol optical and microphysical properties for the two distinct aerosol modes, fine and coarse. The retrieval of height-dependent single scattering albedo data is an additional advantage of GRASP over LIRIC. GRASP also provides an estimation of the systematic and random errors for both the directly retrieved (SD, **RRI, IRI**, SSA) and derived (α, β, VC profiles) aerosol

properties. The single scattering albedo profiles errors are not shown because they are unfortunately not provided at the moment. Additional details on GRASP retrieval algorithm and its performance can be found in Lopatin et al. (2013) and Bovchaliuk et al. (2016).

4 Results

As we commented before, two of the ATR-42 flights, flight number F30 and F31, performed in the framework of ChArMEx-ADRIMED campaign were carried out over Granada region on 16th and 17th June 2013, respectively. Figure 2 shows the time series of the lidar range corrected signal (RCS) **and the depolarization ratio (δ)** at 532 nm on both days measured at Granada station. **The RCS is calculated as P*r^2, where P is the lidar signal (corrected from background and dark current) and r is the altitude.** On the first day, a homogeneous layer is observed from the surface up to 5 km a.s.l., with an elevated aerosol layer coupled to the superficial aerosol layer throughout the day. The next day this layer was decoupled from the aerosol layer close to surface and it disappeared around 13:00 UTC and **measurements of δ evidence that there was an aerosol type below 2.7 km a.s.l. and another aerosol type above this altitude up to 5.5 km a.s.l..** On 16th June, the lidar measurements (marked with purple lines in Fig 2) obtained during the first flight between 14:15 and 14:45 UTC and sun-photometer measurements collected at 16:22 UTC (black dashed line in Fig 2) at Granada and Cerro Poyos were selected for further analysis. The selected sun-photometer measurement was the closest measurement available in time to the first flight. On 17th June, the lidar measurements obtained during the second flight (07:15 to 07:45 UTC) and sun-sky photometer measurements obtained at both stations at 07:40 UTC were selected for further analysis.

AERONET products during these flights indicate the presence of dust particles. In fact, on 16th June; AOD_{440} at 14:15 UTC was around 0.26 and 0.19 for Granada and Cerro Poyos, respectively, and 0.27 and 0.22 at 16:22 UTC. On this day, the $AE_{440-870}$ was 0.30-0.26 (Granada-Cerro Poyos) at 14:30 UTC and 0.34-0.27 (Granada-Cerro Poyos) at 16:22 UTC, indicating moderate atmospheric aerosol load dominated by coarse particles. On 17th June, the AOD_{440} at 07:40 UTC was 0.21 and 0.18 and the $AE_{440-870}$ was 0.43 and 0.30 for Granada and Cerro Poyos, respectively, which also indicates the predominance of coarse particles on this day. The presence of mineral dust over Granada region during both days is confirmed by the analysis of back-trajectories analysis (not shown) by HYSPLIT model (Hybrid Single-Particle Lagrangian Integrated Trajectory; Stein et al., 2015; Rolph, 2016), which indicates that the relevant air masses came from the Saharan region, specifically from Algeria, at different heights.

4.1 Comparison of columnar properties retrieved by GRASP and AERONET algorithms

Some of the aerosol columnar properties obtained from AERONET and retrieved by GRASP (combining photometer and lidar measurements) on 16th and 17th June at Granada and Cerro Poyos stations are shown in Figures 3 to 5 and summarized in Table 3.

Figure 3 shows the column-integrated PSD retrieved by both AERONET and GRASP algorithms on 16th and 17th June for Granada and Cerro Poyos stations. The retrieved PSD evidence the predominance of coarse mode particles, as expected for dust events (Lyamani et al., 2005; Guerrero-Rascado et al, 2009). Both AERONET and GRASP retrieved PSD present a bimodal behavior, with the radius of fine mode below 0.5 µm and the radius of coarse mode above 0.5 µm. The differences between the PSD retrieved by GRASP and AERONET are mostly within uncertainties associated with both methods ($\pm 10 - 35\%$ for the size range from 0.1 µm to 7 µm and $\pm 35 - 100\%$ outside this range; Dubovik et al., 2000) except for the size range 5 - 8.7 µm where the differences are higher, especially at 6.64 µm ($> 100\%$). Furthermore, the coarse mode retrieved

by GRASP over both sites shows a clear shift towards higher radii in comparison to the AERONET retrievals (Figure 3). This shift was also observed by Lopatin et al. (2013) during dust and biomass burning events over Minsk, Belarus and by Bovchaliuk et al. (2016) during dust events over Dakar, Senegal. These authors attributed this coarse mode shift towards higher radii to the use of the lidar data in the GRASP retrievals. The lidar data provide additional information at scattering angles of 180º and further wavelengths compared to the sun-photometer, influencing the size distribution retrieved especially in the coarse mode.

Table 3 summarizes the columnar r_{eff} and VC of fine and coarse modes obtained at both stations by AERONET and GRASP algorithms on 16th and 17th June. The retrieved microphysical properties are similar to those typically obtained during African desert dust events over Granada (Valenzuela et al., 2012b). The fine mode r_{eff} retrieved by both methods ranges between 0.10 and 0.13 µm. Differences between fine mode r_{eff} retrieved by GRASP and AERONET are below 0.02 µm, which are within the uncertainty of the inversions (Lopatin et al., 2013; Torres et al., 2014). For the coarse mode, the r_{eff} values obtained by GRASP were 0.03 µm higher than those retrieved by AERONET but the differences are within the uncertainty range. A similar behavior is observed for the column-integrated volume concentration, with slightly larger values provided by GRASP for the fine and coarse modes (0.016 ±0.003 and 0.148 ±0.017 µm³/µm²) compared to AERONET (0.014 ±0.003 and 0.125 ±0.013 µm³/µm²), but differences are still within the uncertainties.

Figure 4 illustrates the retrieved columnar RRI and IRI for each day obtained by GRASP and AERONET at Granada and Cerro Poyos. Moreover, RRI and IRI at **530** nm estimated by Denjean et al. (2016) using airborne measurements over Granada on 16th and 17th June are included in the plot. AERONET provides RRI and IRI for the whole size distribution, while GRASP is able to provide RRI and IRI for fine and coarse modes separately. The RRI retrieved by GRASP and AERONET algorithms do not show any spectral wavelength variations, and the differences between RRI values retrieved by both inversion algorithms are within the uncertainties (differences below 5%). Because of the predominance of the coarse mode during the analyzed dust event, both the AERONET and airborne RRI values are close to the values retrieved by GRASP for coarse mode, with differences <0.03, on both days. On the other hand, the IRI values retrieved by GRASP for the fine mode present a rather low spectral dependence while IRI values for the coarse mode presents a clear increase in the UV region. These results are coherent with those reported for different absorption species by Schuster et al. (2016) using AERONET data. **At Cerro Poyos we did not find the spectral dependence of the IRI typically associated to mineral dust. The AOD at 440 nm were around 0.18 - 0.27 and we used AERONET level 1.5 products, therefore, these values have large uncertainties (> 50%; Dubovik et al., 2000). The lack of spectral dependence can be just an artifact of the inversion. However, it is worthy to note that at Cerro Poyos the PSD shows a mode in the coarse mode size range around 1 µm. As there is still discussion in the scientific community about dust RI and about the differences in dust particles between different sources (e.g. Colarco et al., 2014), results can suggest possible differences in dust RI between long range transported and mixture with local dust injections (the area is very dry in summer, thus favoring local mineral dust resuspension) and local pollution.** The RRI and IRI values provided by AERONET show good agreement with GRASP retrievals for coarse mode, something expected due to the large predominance of dust particles. Better agreement between IRI retrieved by AERONET and by GRASP for coarse mode was found for Cerro Poyos, with differences ~ 10%, while for Granada these differences are between 35 - 80% (larger differences for lower wavelengths). The high discrepancy between IRI retrieved by AERONET and by GRASP in the case of Granada can be explained by the uncertainty associated to the incomplete lidar overlap. Cerro Poyos station is located above the lidar incomplete overlap height, and thus the effect of the incomplete overlap on the retrieval is negligible. This is not the case for the retrieval from Granada station. On 16th June, IRI airborne values estimated at **530** nm are close to

IRI retrieved by GRASP at 532 nm for coarse mode, and the differences are within the associated uncertainties. On the other hand, on 17th June, there are more differences between IRI values retrieved by GRASP at Granada station and those estimated from airborne measurement, with differences over 100%, whereas for the Cerro Poyos retrievals the differences are 50%.

5   Figure 5 shows the columnar SSA values retrieved by GRASP and AERONET on 16th and 17th June at Granada and Cerro Poyos. **Moreover, the SSA value at 530 nm calculated by Denjean et al. (2016) for dust layer using airborne measurements during the campaign was 0.95 ±0.04. SSA retrieved by GRASP at 532 nm are close to the airborne value. Better agreement with this value is found for the retrievals from Granada on 16th June and at Cerro Poyos on 17th June. The differences from Granada on 17th June could be due the in-situ value was calculated for the dust**

10   **layer whereas that GRASP and AERONET use sun-photometer data, which measures the total atmospheric column. Furthermore, in the case of Granada station, these measures could be influenced by injections of local pollution. The retrieved SSA values are in the range between 0.85-0.98 (355-1064 nm wavelength range) and are in the ranges** of the typical values for dust aerosols (Dubovik et al., 2002; Toledano et al., 2011; Lopatin et al., 2013). Both AERONET and GRASP retrievals follow the same pattern with wavelength, with increasing SSA as wavelength increases,

15   which is a typical characteristic of dust aerosols (Dubovik et al., 2002; Valenzuela et al., 2012b). Differences between SSA retrieved by AERONET and GRASP algorithms are below 0.03 at all wavelengths, within the uncertainties associated with each method. The discrepancies between SSA retrieved by AERONET and GRASP algorithms are obtained for Cerro Poyos station (< 1 %) in particular at 1020 nm, whereas for Granada retrievals the differences are bigger and the lowest discrepancies are obtained at 675 nm.

20   **4.2 Comparison of vertical properties retrieved by GRASP and LIRIC algorithms and in situ airborne measurements**

Figure 6 shows particle VC profiles for the fine, coarse and total (fine+coarse) modes, retrieved by GRASP and LIRIC, together with the results obtained with airborne instrumentation. Generally, there is good agreement between the profiles retrieved by GRASP and LIRIC and those obtained by the airborne instrumentation, with both retrievals and the airborne

25   data reproducing similar vertical structures on both days. The airborne data show a larger variability compared to GRASP and LIRIC mostly associated to their larger uncertainty and the fact that the airborne data are instantaneous measurements whereas the lidar data are an average over a 30-minute period.

Table 4 summarizes the volume concentration mean values and associated standard deviations retrieved from the in-situ airborne measurements, GRASP and LIRIC profiles shown in Figure 6. Data are analyzed only for those layers with total

30   volume concentration above 20 $\mu m^3/cm^3$ to avoid undesirable outliers for low aerosol loads. Hence for 16th June we analyze the layer between 1.2 and 4.5 km a.s.l. and for 17th June, the analyzed layer is that from 2.6 to 5.0 km a.s.l.. There is a slight contribution of the fine mode in the dust layers on both days, with values between 3 $\mu m^3/cm^3$ for the airborne data and 5.3 $\mu m^3/cm^3$ for LIRIC. In general, it is observed that the coarse mode contributes the most to the total VC, as expected due to the predominance of mineral dust. Coarse mode concentration values range between 28 ±4 and 46 ±4 $\mu m^3/cm^3$ on June16

35   and 35 ±5 and 42 ±11 $\mu m^3/cm^3$ on June 17, depending on the dataset considered. GRASP and LIRIC retrievals both overestimate the airborne data for the fine mode while they overestimate/underestimate the total mode on 16th/17th June using sun-photometer data at both Granada and Cerro Poyos stations. In the case of fine mode, the differences between the airborne and the retrievals are lower than 5 $\mu m^3/cm^3$ (about 80%). The agreement for the coarse mode is high with differences lower than 6 $\mu m^3/cm^3$ (25%), except for the LIRIC inversion from Cerro Poyos on 16 June, where the difference

40   is 19 $\mu m^3/cm^3$ (around 80%). Both algorithms show the largest differences for the retrievals from Cerro Poyos on 16th June,

whereas the differences for the retrievals from Granada for total and coarse mode are around 15% and 25% using GRASP and LIRIC, respectively. **On 17th June for Granada retrieval, the differences between both algorithms and airborne data below 2 km a.s.l. could be explained because the flight was not exactly over Granada city as shown in Fig. 1 and in the first two kilometers of the atmosphere differences are expected because of the influence of the city.** In the dust layer on 17th June, the differences are around 20% for coarse and total volume concentration by both algorithms for Granada and Cerro Poyos stations. Differences between GRASP and LIRIC retrievals are below 30%, well within the combined uncertainty from both retrievals. There are no accurate calculations of the uncertainty associated to LIRIC profiles, but it is estimated to be around 50% in cases of mineral dust (Granados-Muñoz et. al., 2016).

Figure 7 shows the aerosol β coefficient profiles at 355, 532 and 1064 nm retrieved by GRASP and the profiles calculated by Klett-Fernald method. **The LR used in Klett method is assumed constant for the entire profile and was computed by fitting the integral of the different extinction profiles to the measured aerosol optical depth. However, GRASP uses both sun-sky radiances and the backscatter lidar data to provide LR values, both in column-integrated and vertical profiles.** The GRASP LR values are close to the LR values used by Klett-Fernald method, these values are typical from Saharan dust measured over the southeastern Spain (Guerrero-Rascado et al., 2009; Navas-Guzmán et al., 2013).

Below 1.6 km, the Klett retrieval at 355 showed unrealistic values probably associated with instrumental problems. However, for GRASP this problem does not appear and seems to be canceled due to the use of the combined data of lidar and sun-photometer. GRASP algorithm underestimates the values obtained by Klett-Fernald method, except for Cerro Poyos retrieval on 17th June, with larger differences for Granada retrievals. Nevertheless, the differences are within the uncertainties claimed for our system (approximately 30%). The differences at the ultraviolet channel reached 19% and around 9% for Granada and Cerro Poyos retrievals, respectively. The discrepancies between backscatter coefficient profiles at 532 nm retrieved by GRASP and Klett-Fernald are around 16% for Granada retrieval on 16th June and 11% on 17th June and for Cerro Poyos retrievals on both days. In the case of backscatter coefficient profiles at 1064 nm, the differences between both retrievals are close to 24% for Granada on 16th June and Cerro Poyos on 17th June, while for the other two cases the differences are the lowest (6%).

The comparison between aerosol α coefficient profiles retrieved by GRASP and those measured by airborne instruments (CAPS and PLASMA) is shown in Figure 8. Profiles retrieved by GRASP show good agreement with the CAPS data (measurements only on 16th June at 532 nm), even though with slightly higher values for GRASP of approximately 3 ±3 Mm^{-1} (7%) and 9 ±5 Mm^{-1} (18%) for the inversions from Granada and Cerro Poyos, respectively. GRASP extinction coefficient retrievals were larger than PLASMA measurements at all wavelengths, with larger differences at the ultraviolet channel (~50%). On 16th June, the differences for the ultraviolet channel are 20 ±11 Mm^{-1} (45%) and for the visible and ultraviolet channels are 11 ±8 Mm^{-1} (30% and 40%, respectively). These differences were similar or lower than those obtained by Karol et al. (2013) when comparing PLASMA with lidar data. On 17th June, PLASMA and GRASP show the same layers, but their differences are larger, reaching 50% for the visible channel and more than 60% for the ultraviolet and infrared channels. As GRASP and LIRIC reproduce the same layer structures for volume concentrations, these differences can be mainly associated with PLASMA.

Vertical profiles of SSA obtained by GRASP at Granada and Cerro Poyos station on 16th and 17th June are shown in Figure 9. As SSA is an intensive aerosol parameter, only SSA values for the layers with large aerosol loads are represented. On 16th June, there are no remarkable changes in SSA with altitude, which agrees with the extinction and backscatter coefficients profiles and with the particle volume concentrations. For 17th June, vertical profiles of SSA are sensitive to the different aerosol layers with different aerosol types illustrating the capabilities of GRASP for detecting different aerosol

layers with different composition. Nonetheless, the values of SSA are also within those associated with dust aerosol in previous studies (Dubovik et al., 2002; Toledano et al., 2011; Lopatin et al., 2013). Differences are observed again between the SSA profiles obtained at Granada and Cerro Poyos stations. On 16th June SSA differences between both retrievals are lower than 2% while on 17th differences reach up to 10%. This result is again associated with overlap issues, although the influence of the city with injection of large amounts of particles confined below the altitude of Cerro Poyos cannot be neglected in sky radiance measurements.

Figure 10 shows scattering AE computed between 450 and 700 nm, AE_{sca} (450-700), obtained by GRASP algorithm at Granada and Cerro Poyos stations together with those obtained from nephelometer airborne measurements. GRASP scattering coefficient profiles are calculated by multiplying the extinction coefficient by the SSA at the same wavelength. Despite the fact that the AE_{sca} (450-700) profiles from the airplane date are noisier than GRASP profiles, general good agreement is observed, with discrepancies within the uncertainties. In general, GRASP values are larger than the airborne data for altitudes above 2.5 km a.s.l.. Above this altitude, the AE_{sca} (450-700) values are close to zero for the airborne data on both days, which is typical of aerosols dominated by coarse particles (Bergstrom et al., 2007). However, in the lower part of the profiles AE_{sca} (450-700) values are larger (~0.7 and ~1.6 for the airborne data on 16th and 17th June, respectively) and GRASP profiles underestimate the airborne data. The values for these lower altitudes, including those retrieved by GRASP using the sun-photometer data measured at Granada and the airborne data, were similar to in-situ measurements at IISTA-CEAMA, with values around 0.70 ±0.10 and 1.67 ±0.07 on 16th and 17th June, respectively. GRASP profiles have similar values above and below 2.5 km a.s.l. with better agreement between airborne data and Cerro Poyos retrieval. Granada retrieval shows more differences on 17th June, the case with aerosol layers with different aerosol types. **On 17th June, in the range ~1.8 – 2.7 km a.s.l. the aerosol load was low (~5 $\mu m^3/cm^3$) and, hence, SSA and AE values could be less reliable in this layer. However, the layer up to 1.8 km a.s.l. showed a concentration moderate (~17 $\mu m^3/cm^3$) with a different composition to layer above 2.7 km a.s.l. as show the SSA and AE profiles.**

Finally, the Table 5 shows the mean values with ±1 standard deviation of β-AE (532-1064) and color ratio (CR $=\beta(532\,nm)/\beta(1064\,nm)$) calculated by GRASP in the layer between 1.8 and 4.5 km a.s.l. and between 2.8 and 5.0 km a.s.l. on 16th and 17th June, respectively. The values of β-AE and CR are 0.5 ±0.2 and 1.3 ±0.3, respectively, are in the range of typical values for dust aerosols (Perrone et al., 2014).

5 Summary and conclusion

GRASP algorithm is applied to lidar and sun-sky photometer measurements at Granada during the ChArMEx-ADRIMED campaign in summer 2013. **Data from a second photometer at 1.2 km above the lidar system are also used, locate it above the lidar incomplete overlap height.** This second sun-photometer allows us to explore the effect of the lidar incomplete overlap on the retrievals and the influence of the aerosol vertical layering on the results, especially in cases of complex structures when different aerosol types are observed below and above Cerro Poyos. The optical and microphysical properties retrieved by GRASP using independent AERONET data have been compared with airborne measurements corresponding to two flights.

The flights took place on 16th and 17th June, 2013, during dust events affecting Granada. The GRASP retrievals show a good agreement with AERONET products, with discrepancies well below the uncertainties. Total volume concentration profiles retrieved by GRASP and airborne measurements show a good agreement with differences around 15% on 16[th]June using for the retrieval sun-photometer data measured at Granada and on 17[th]June using for the retrieval sun-photometer

data measured at Cerro Poyos. The agreement for the aerosol backscatter profiles with respect to those obtained using only lidar data and Klett-Fernald algorithm are quite good using both station data, showing differences below 12% at 355 and 532 nm for Cerro Poyos. In the case of the aerosol extinction profiles, good agreement was found between GRASP and the CAPS data (differences below 20%), while the comparison with PLASMA data shows larger differences. The SSA profiles show values typical of dust aerosols and the differences between retrievals using sun-photometer data measured at Granada and Cerro Poyos are below 10% at the lidar wavelengths. Other aerosol properties obtained with GRASP, like the color ratio and the backscatter - Angström Exponent, also show similar values to those observed in the literature for dust aerosols. GRASP algorithm is quite robust as shows the agreement between the optical and microphysical properties retrieved by AERONET products and airborne measurements. Results obtained here show that the combination of lidar and sun-photometer data can provide improved and more complete column-integrated data compared to AERONET retrieval. Reliable vertically-resolved properties such as the SSA, extinction or volume concentration are also provided, improving the capabilities of previous algorithms such as LIRIC.

Nonetheless, the retrieved scattering-Angström exponent profiles together with the better agreement found between Cerro Poyos retrievals and the aircraft compared to Granada retrievals indicate that GRASP vertical distribution of some of the aerosol properties is still affected by considerable uncertainties. This is somehow an expected result because of the use of the column-integrated sun-photometer data.

The analysis presented here is useful as a primary evaluation of the GRASP algorithm using sun-photometer and lidar signal to retrieve aerosol microphysical properties, both integrated along the vertical column and as vertical profiles. The use of a second sun-photometer located over the local atmospheric boundary layer can be very relevant for the study of the properties of aerosol layers with features really different than the atmospheric boundary layer aerosol. However, the presented analysis is representative of Saharan dust transport to south Europe and still it is necessary to use a more complete dataset that includes different aerosol loads and types. In future studies, we could try to use of the combination of one lidar with two sun-sky photometers at different height to try improve the retrievals in the cases with different aerosol layers. In addition, in order to validate the presented GRASP scheme, in the future it is planned to use global aerosol models (e.g. GEOS-5) following an approach similar to Whiteman et al., (2017).

References

Alados-Arboledas, L., Muller, D., Guerrero-Rascado, J. L., Navas-Guzman, F., Pérez-Ramírez, D., and Olmo, F. J.: Optical and microphysical properties of fresh biomass burning aerosol retrieved by Raman lidar, and star-and sun-photometry, Geophys. Res. Lett., 38, L01807, doi:10.1029/2010gl045999, 2011.

Ansmann, A., Riebesell, M., Wandinger, U., Weitkamp, C., Voss, E., Lahmann W., and Michaelis, W.: Combined Raman elastic backscatter LIDAR for vertical profiling of moisture, aerosol extinction, backscatter, and LIDAR ratio, Appl. Phys., B55, 18– 28, doi:10.1007/BF00348608, 1992.

Barreto, Á., Cuevas, E., Granados-Muñoz, M.-J., Alados-Arboledas, L., Romero, P. M., Gröbner, J., Kouremeti, N., Almansa, A. F., Stone, T., Toledano, C., Román, R., Sorokin, M., Holben, B., Canini, M., and Yela, M.: The new sun-sky-lunar Cimel CE318-T multiband photometer – a comprehensive performance evaluation, Atmos. Meas. Tech., 9, 631-654, doi:10.5194/amt-9-631-2016, 2016.

Barreto, Á., Román, R., Cuevas, E., Berjón, A. J., Almansa, A. F., Toledano, C., González, R., Hernández, Y., Blarel, L., Goloub, P., and Yela, M.: Assessment of nocturnal Aerosol Optical Depth from lunar photometry at Izaña high mountain Observatory, Atmos. Meas. Tech. Discuss., https://doi.org/10.5194/amt-2016-423, in review, 2017.

Baumgardner, D., Dye, J. E., Gandrud, B. W., and Knollenberg, R. G.: Interpretation of measurements made by the Forward Scattering Spectrometer Probe (FSSP-300) during the Airborne Arctic Stratospheric Expedition, J. Geophys. Res., 97, 8035-8046, DOI: 10.1029/91JD02728, 1992.

Bergstrom, R. W., Pilewskie, P., Russell, P. B., Redemann, J., Bond, T. C., Quinn, P. K., and Sierau, B.: Spectral absorption properties of atmospheric aerosols, Atmos. Chem. Phys., 7, 5937-5943, doi:10.5194/acp-7-5937-2007, 2007.

Böckmann, C.: Hybrid regularization method for the ill-posed inversion of multiwavelength lidar data to determine aerosol size distributions, Appl. Optics, 40, 1329-1342, 2001.

Boucher, O., Randall, D., Artaxo, P., Bretherton, C., Feingold, G., Forster, P., Kerminen, V.-M., Kondo, Y., Liao, H., Lohmann, U., Rasch, P., Satheesh, S. K., Sherwood, S., Stevens, B., and Zhang, X. Y.: Clouds and Aerosols, in: Climate Change 2013: The Physical Science Basis. Contribution of Working Group I to the Fifth Assessment Report of the Intergovernmental Panel on Climate Change, edited by: Stocker, T. F., Qin, D., Plattner, G.-K., Tignor, M., Allen, S. K., Boschung, J., Nauels, A., Xia, Y., Bex, V., and Midgley, P. M., Cambridge University Press, Cambridge, United Kingdom and New York, USA, 571–657, 2013.

Bovchaliuk, V., Goloub, P., Podvin, T., Veselovskii, I., Tanre, D., Chaikovsky, A., Dubovik, O., Mortier, A., Lopatin, A., Korenskiy, M., and Victori, S.: Comparison of aerosol properties retrieved using GARRLiC, LIRIC, and Raman algorithms applied to multi-wavelength lidar and sun/sky-photometer data, Atmos. Meas. Tech., 9, 3391-3405, doi:10.5194/amt-9-3391-2016, 2016.

Bravo-Aranda, J. A., Navas-Guzmán, F., Guerrero-Rascado, J. L., Pérez-Ramírez, D., Granados-Muñoz, M. J., and Alados-Arboledas, L.: Analysis of lidar depolarization calibration procedure and application to the atmospheric aerosol characterization, Int. J. Remote Sens., 34(9–10), 3543–3560, 2013.

Bravo-Aranda, J. A., Titos, G., Granados-Muñoz, M.J., Guerrero-Rascado, J. L., Navas-Guzmán, F., Valenzuela, A., Lyamani, H., Olmo, F. J., Andrey, J., and Alados-Arboledas, L.: Study of mineral dust entrainment in the planetary boundary layer by lidar depolarization technique, Tellus B, 67, 26180, doi:10.3402/tellusb.v67.26180, 2015.

Cai, Y., Montague, D. C., Mooiweer-Bryan, W., and Deshler, T.: Performance characteristics of the ultra-high sensitivity aerosol spectrometer for particles between 55 and 800 nm: Laboratory and field studies, J. Aerosol Sci., 39, 759–769, 2008.

Calvo, A.I., Olmo, F.J., Lyamani, H., Alados-Arboledas, L., Castro, A., Fernández-Raga, M., Fraile, R.: Chemical composition of wet precipitation at the background EMEP station in Víznar (Granada, Spain) (2002-2006). Atmos. Res. 96 (2-3), 408–420, 2010.

Chaikovsky, A., Dubovik, O., Goloub, P., Balashevich, N., Lopatsin, A., Karol, Y., Denisov, S. and Lapyonok, T.: Software package for the retrieval of aerosol microphysical properties in the vertical column using combined lidar/photometer data (test version), Technical Report, Minsk, Belarus, Institute of Physics, National Academy of Sciences of Belarus, 2008.

Chaikovsky, A., Dubovik, O., Goloub, P., Tanré, D.,Pappalardo, G., Wandinger, U., Chaikovskaya, L., Denisov, S., Grudo, Y., Lopatsin, A., Karol, Y., Lapyonok, T., Korol, M., Osipenko, F., Savitski, D., Slesar, A., Apituley, A., Arboledas, L. A.,Binietoglou, I., Kokkalis, P., Granados Muñoz, M. J., Papayannis, A., Perrone, M. R., Pietruczuk, A., Pisani, G., Rocadenbosch, F., Sicard, M., De Tomasi, F., Wagner, J., and Wang, X.: Algorithm and software for the retrieval of vertical aerosol properties using combined lidar/radiometer data: dissemination in EARLINET, 26th International Laser and Radar Conference, Porto Heli, Greece, 2012.

Chaikovsky, A., Dubovik, O., Holben, B., Bril, A., Goloub, P., Tanré, D., Pappalardo, G., Wandinger, U., Chaikovskaya, L., Denisov, S., Grudo, J., Lopatin, A., Karol, Y., Lapyonok, T., Amiridis, V., Ansmann, A., Apituley, A., Allados-Arboledas, L., Binietoglou, I., Boselli, A., D'Amico, G., Freudenthaler, V., Giles, D., Granados-Muñoz, M. J., Kokkalis, P., Nicolae, D., Oshchepkov, S., Papayannis, A., Perrone, M. R., Pietruczuk, A., Rocadenbosch, F., Sicard, M., Slutsker, I., Talianu, C., De Tomasi, F., Tsekeri, A., Wagner, J., and Wang, X.: Lidar-Radiometer Inversion Code (LIRIC) for the retrieval of vertical aerosol properties from combined lidar/radiometer data: development and distribution in EARLINET, Atmos. Meas. Tech., 9, 1181-1205, doi:10.5194/amt-9-1181-2016, 2016.

Colarco, P.R., Nowottnick, E.P., Randles, C.A., Yi, B., Yang, P., Kim, K.-M., Smith, J.A., and Bardeen, C.: Impact of radiatively interactive dust aerosols in the NASA GEOS-5 climate model: Sensitivity to dust particle shape and refractive index. J. Geophys. Res., 119, 753-786, doi: 10.1002/2013JD020046. 2014.

Córdoba-Jabonero, C., Sorribas, M., Guerrero-Rascado, J. L., Adame, J. A., Hernández, Y., Lyamani, H., Cachorro, V., Gil, M., Alados-Arboledas, L., Cuevas, E., and de la Morena, B.: Synergetic monitoring of Saharan dust plumes

and potential impact on surface: a case study of dust transport from Canary Islands to Iberian Peninsula, Atmos. Chem. Phys., 11, 3067-3091, doi:10.5194/acp-11-3067-2011, 2011.

Denjean, C., Cassola, F., Mazzino, A., Triquet, S., Chevaillier, S., Grand, N., Bourrianne, T., Momboisse, G., Sellegri, K., Schwarzenbock, A., Freney, E., Mallet, M., and Formenti, P.: Size distribution and optical properties of mineral dust aerosols transported in the western Mediterranean, Atmos. Chem. Phys., 16, 1081-1104, doi:10.5194/acp-16-1081-2016, 2016.

Dubovik, O. and King, M.: A flexible inversion algorithm for retrieval of aerosol optical properties from Sun and sky radiance measurements, J. Geophys. Res., 105, 20673–20696, doi:10.1029/2000JD900282, 2000.

Dubovik, O., Smirnov, A., Holben, B. N., King, M., Kaufman, Y. J., Eck, T. F., and Slutsker, I.: Accuracy assessments of aerosol optical properties retrieved from Aerosol Robotic Network (AERONET) sun and sky radiance measurements, J. Geophys. Res., 105, 9791–9806, 2000.

Dubovik, O., Holben, B., Eck, T., Smirnov, A., Kaufman, Y., King, M., Tanre, D., and Slutsker, I.: Variability of absorption and optical properties of key aerosol types observed in worldwide locations, J. Atmos. Sci., 59, 590–608, 2002.

Dubovik, O., Sinyuk, A., Lapyonok, T., Holben, B. N., Mishchenko, M., Yang, P., Eck, T. F., Volten, H., Munoz, O., Veihelmann, B., van der Zande, W. J., Leon, J.-F., Sorokin, M., and Slutsker, I.: Application of spheroid models to account for aerosol particle nonsphericity in remote sensing of desert dust, J. Geophys. Res., 111, D11208, doi:10.1029/2005JD006619, 2006.

Dubovik, O., Herman, M., Holdak, A., Lapyonok, T., Tanre, D., Deuze, J. L., Ducos, F., Sinyuk, A., and Lopatin, A.: Statistically ´ optimized inversion algorithm for enhanced retrieval of aerosol properties from spectral multi-angle polarimetric satellite observations, Atmos. Meas. Tech., 4, 975–1018, doi:10.5194/amt-4- 975-2011, 2011.

Dulac, F.: An overview of the Chemistry-Aerosol Mediterranean Experiment (ChArMEx), European Geosciences Union General Assembly, Geophysical Research Abstracts Vol. 16, EGU2014-11441, 27 April–2 May 2014, Vienna, Austria, 2014.

Eck, T. F., Holben, B. N., Reid, J. S., Dubovik, O., Smirnov, A., O'Neill, N. T., Slutsker, I., and Kinne, S.: Wavelength dependence of the optical depth of biomass burning, urban, and desert dust aerosols, J. Geophys. Res., 104, 31,333–31,349, doi:10.1029/1999JD900923, 1999.

Fernald, F. G.: Analysis of atmospheric lidar observations- Some comments, App. Optics, 23, 652–653, 1984.

Fernald, F. G., Herman, B. M., and Reagan, J. A.: Determination of aerosol height distributions by lidar, J. Appl. Meteorol., 11, 482–489, 1972.

Franke, K., A. Ansmann, D. Müller, D. Althausen, F. Wagner, and R. Scheele, One-year observations of particle lidar ratio over the tropical Indian Ocean with Raman lidar, Geophys. Res. Lett., 28, 4559–4562, doi:10.1029/2001GL013671, 2001.

Granados-Muñoz, M. J., Guerrero-Rascado, J. L., Bravo-Aranda, J. A., Navas-Guzmán, F., Valenzuela, A., Lyamani, H., Chaikovsky, A., Wandinger, U., Ansmann, A., Dubovik, O., Grudo, J., and Alados-Arboledas, L.: Retrieving aerosol microphysical properties by Lidar-Radiometer Inversion Code (LIRIC) for different aerosol types, J. Geophys. Res., 119, 4836–4858, doi:10.1002/2013JD021116, 2014.

Granados-Muñoz, M. J., Bravo-Aranda, J. A., Baumgardner, D., Guerrero-Rascado, J. L., Pérez-Ramírez, D., Navas-Guzmán, F., Veselovskii, I., Lyamani, H., Valenzuela, A., Olmo, F. J., Titos, G., Andrey, J., Chaikovsky, A., Dubovik, O., Gil-Ojeda, M., and Alados-Arboledas, L.: A comparative study of aerosol microphysical properties retrieved from ground-based remote sensing and aircraft in situ measurements during a Saharan dust event, Atmos. Meas. Tech., 9, 1113-1133, doi:10.5194/amt-9-1113-2016, 2016.

Guerrero-Rascado, J. L., Ruiz, B., and Alados Arboledas, L.: Multispectral Lidar characterization of the vertical structure of Saharan dust aerosol over southern Spain, Atmos. Environ., 42, 2668– 2681, doi:10.1016/j.atmosenv.2007.12.062, 2008.

Guerrero-Rascado, J. L., Olmo, F. J., Avilés-Rodríguez, I., Navas-Guzmán, F., Pérez-Ramírez, D., Lyamani, H., and Alados Arboledas, L.: Extreme Saharan dust event over the southern Iberian Peninsula in september 2007: active and passive remote sensing from surface and satellite, Atmos. Chem. Phys., 9, 8453-8469, doi:10.5194/acp-9-8453-2009, 2009.

Guerrero-Rascado, J.L., Landulfo, E., Antuña, J.C., Barbosa, H.M.J., Barja, B., Bastidas, A.E., Bedoya, A.E., da Costa, R.F., Estevan, R., Forno, R.N., Gouveia, D.A., Jimenez, C., Larroza, E.G., Lopes, F.J.S., Montilla-Rosero, E., Moreira, G.A., Nakaema, W.M., Nisperuza, D., Alegria, D., Múnera, M., Otero, L., Papandrea, S., Pawelko, E., Quel, E.J., Ristori, P., Rodrigues, P.F., Salvador, J., Sánchez, M.F., Silva, A.: Latin American Lidar Network (LALINET) for aerosol research: diagnosis on network instrumentation. J Atmos. Sol. Terr. Phys. 138–139, 112–120, 2016.

Grund, C. J., and Eloranta, E. W.: University of Wisconsin high spectral resolution lidar. Opt. Eng., 30, 6–12, doi:10.1117/12.55766, 1991.

Holben, B. N., Eck, T. F., Slutsker, I., Tanre, D., Buis, J. P., Setzer, A., Vermote, E., Reagan, J. A., Kaufman, Y. J., Nakajima, T., Lavenu, F., Jankowiak, I., and Smirnov, A.: AERONET-a federated instrument network a data archive for aerosol characterization, Remote Sens. Environ., 66, 1- 16, 1998.

IPCC: Contribution of Working Group I to the Fifth Assessment Report of the Intergovernmental Panel on Climate Change, Summary for Policymakers in Climate Change, Stocker, Cambridge University Press, 2013.

Klett, J. D.: Stable analytical inversion solution for processing lidar returns, Appl. Optics, 20, 211–220, 1981.

Klett, J. D.: Lidar inversion with variable backscatter/extinction ratios, Appl. Optics, 24, 1638–1643, 1985.

Karol, Y., Tanré, D., Goloub, P., Vervaerde, C., Balois, J. Y., Blarel, L., Podvin, T., Mortier, A., and Chaikovsky, A.: Airborne sun photometer PLASMA: concept, measurements, comparison of aerosol extinction vertical profile with lidar, Atmos. Meas. Tech., 6, 2383–2389, doi:10.5194/amt-6-2383-2013, 2013.

Lewis, J. R., Campbell, J. R., Welton, E. J., Stewart, S. A., and Haftings, P. C.: Overview of MPLNET version 3 cloud detection, J. Atmos. Ocean. Tech., 33, 2113–2134, 2016.

Lopatin, A., Dubovik, O., Chaikovsky, A., Goloub, P., Lapyonok, T., Tanré, D., and Litvinov, P.: Enhancement of aerosol characterization using synergy of lidar and sun-photometer coincident observations: the GARRLiC algorithm, Atmospheric Measurement Techniques, 6, 2065–2088, doi:10.5194/amt-6-2065-2013, 2013.

Lyamani, H., Olmo, F. J., and Alados-Arboledas, L.: Saharan dust outbreak over southeastern Spain as detected by sun photometer, Atmos. Environ., 39, 7276–7284, doi:10.1016/j.atmosenv.2005.09.011, 2005.

Lyamani, H., Olmo, F. J., Alcantara, A., and Alados-Arboledas, L.: Atmospheric aerosols during the 2003 heat wave in southeastern spain I: Spectral optical depth, Atmos. Environ., 40, 6453–6464, doi.org/10.1016/j.atmosenv.2006.04.048 , 2006.

Lyamani, H., Fernández-Gálvez, J., Pérez-Ramírez, D., Valenzuela, A., Antón, M., Alados, I., Titos, G., Olmo, F. J., and Alados- Arboledas, L.: Aerosol properties over two urban sites in South Spain during an extended stagnation episode in winter season, Atmos. Environ., 62, 424–432, doi.org/10.1016/j.atmosenv.2012.08.050, 2012.

Mallet, M., Dulac, F., Formenti, P., Nabat, P., Sciare, J., Roberts, G., Pelon, J., Ancellet, G., Tanré, D., Parol, F., Denjean, C., Brogniez, G., di Sarra, A., Alados-Arboledas, L., Arndt, J., Auriol, F., Blarel, L., Bourrianne, T., Chazette, P., Chevaillier, S., Claeys, M., D'Anna, B., Derimian, Y., Desboeufs, K., Di Iorio, T., Doussin, J.-F., Durand, P., Féron, A., Freney, E., Gaimoz, C., Goloub, P., Gómez-Amo, J. L., Granados-Muñoz, M. J., Grand, N., Hamonou, E., Jankowiak, I., Jeannot, M., Léon, J.-F., Maillé, M., Mailler, S., Meloni, D., Menut, L., Momboisse, G., Nicolas, J., Podvin, T., Pont, V., Rea, G., Renard, J.-B., Roblou, L., Schepanski, K., Schwarzenboeck, A., Sellegri, K., Sicard, M., Solmon, F., Somot, S., Torres, B., Totems, J., Triquet, S., Verdier, N., Verwaerde, C., Waquet, F., Wenger, J., and Zapf, P.: Overview of the Chemistry-Aerosol Mediterranean Experiment/Aerosol Direct Radiative Forcing on the Mediterranean Climate (ChArMEx/ADRIMED) summer 2013 campaign, Atmos. Chem. Phys., 16, 455-504, doi:10.5194/acp-16-455-2016, 2016.

Massoli, P., Kebabian, P. L., Onasch, T. B., Hills, F. B., and Freedman, A.: Aerosol light extinction measurements by Cavity Attenuated Phase Shift (CAPS) Spectroscopy: Laboratory validation and field deployment of a compact aerosol particle extinction monitor, Aerosol Sci. Tech., 44, 428–435, doi:10.1080/02786821003716599, 2010.

Miffre, A., David, G., Thomas, B., and Rairoux, P.: Atmospheric non-spherical particles optical properties from UV-polarization lidar and scattering matrix, Geophys. Res. Lett., 38, L16804, doi:10.1029/2011GL048310, 2011.

Müller, D., Wandinger, U., and Ansmann, A.: Microphysical particle parameters from extinction and backscatter lidar data by inversion with regularization: simulation, Appl. Opt. 38, 2358-2368, 1999.

Muller, D., Heinold, B., Tesche, M., Tegen, I., Althausen, D.: Amiridis, V., Amodeo, A., Ansmann, A., Alados-Arboledas, L., Balis, D., Comeron, A., D'Amico, G., Gerasopoulos, E., ´Guerrero-Rascado, J. L., Freudenthaler, V., Giannakaki, E., Heese, B., Iarlori, M., Mamouri, R. E., Mona, L., Papayannis, A., Pappalardo, G., Perrone, M. R., Pisani, G., Rizi, V., Sicard, M., Spinelli, N., and Tafuro, A.: EARLINET Observations of the 14–22-May long-range dust transport event during SAMUM 2006: Validation of results from dust transport modelling, Tellus, 61B, 325–339, doi: 10.1111/j.1600-0889.2008.00400.x, 2009.

Müller, T., Laborde, M., Kassell, G., and Wiedensohler, A.: Design and performance of a three-wavelength LED-based total scatter and backscatter integrating nephelometer, Atmos. Meas. Tech., 4, 1291–1303, doi:10.5194/amt-4-1291-2011, 2011.

Murayama, T., Müller, D., Wada, K., Shimizu, A., Sekiguchi, M., and Tsukamoto, T.: Characterization of Asian dust and Siberian smoke with multiwavelength Raman lidar over Tokyo, Japan in spring 2003, Geophys. Res. Lett., 31, L23103, doi:10.1029/2004GL021105, 2004.

Nakajima, T., Tonna, G., Rao, R., Boi, P., Kaufman, Y., and Holben, B.: Use of sky brightness measurements from ground for remote sensing of particulate polydispersions, Applied Optics, 35(15), 2672-2686, doi:10.1364/AO.35.002672, 1996.

Navas-Guzmán, F., Guerrero-Rascado, J. L., and Alados-Arboledas, L.: Retrieval of the lidar overlap function using Raman signals, Opt. Pura Apl., 44, 71–75, 2011.

Navas-Guzmán, F., Bravo-Aranda, J., Guerrero-Rascado, J., Granados-Muñoz, M., and Alados-Arboledas, L.: Statistical analysis of aerosol optical properties retrieved by Raman lidar over Southeastern Spain, Tellus B, 65, 21234, doi:10.3402/tellusb.v65i0.21234, 2013.

Navas-Guzmán, F., Fernández-Gálvez, J., Granados-Muñoz, M. J., Guerrero-Rascado, J. L., Bravo-Aranda, J. A. and Alados-Arboledas, L.: Tropospheric wáter vapour and relative humidity profiles from lidar and microwave radiometry, Atmos. Meas. Tech., 7, 1201-1211, doi:10.5194/amt-7-1201-2014, 2014.

Olmo, F. J., Quirantes, A., Alcántara, A., Lyamani, H., and Alados-Arboledas, L.: Preliminary results of a non-spherical aerosol method for the retrieval of the atmospheric aerosol optical properties, Journal of Quantitative Spectroscopy and Radiative Transfer, 100(1), 305-314, doi:10.1016/j.jqsrt.2005.11.047, 2006.

Olmo, F. J., Quirantes, A., Lara, V., Lyamani, H., and Alados-Arboledas, L.: Aerosol optical properties assessed by an inversion method using the solar principal plane for non-spherical particles, J. Quant. Spectrosc. Radiat. Transfer., 109, 1504–1516, 2008.

Ortiz-Amezcua, P., Guerrero-Rascado, J. L., Granados-Muñoz, M. J., Bravo-Aranda, J. A., and Alados-Arboledas, L.: Characterization of atmospheric aerosols for a long range transport of biomass burning particles from Canadian forest fires over the southern Iberian Peninsula in July 2013, Óptica Pura y Aplicada, 47(1), 43-49, doi:10.1016/j.jqsrt.2007.12.019, 2014.

5   Ortiz-Amezcua, P., Guerrero-Rascado, J. L., Granados-Muñoz, M. J., Benavent-Oltra, J. A., Böckmann, C., Samaras, S., Stachlewska, I. S., Janicka, Ł., Baars, H., Bohlmann, S., and Alados-Arboledas, L.: Microphysical characterization of long-range transported biomass burning particles from North America at three EARLINET stations, Atmos. Chem. Phys., 17, 5931-5946, doi:10.5194/acp-17-5931-2017, 2017.

Pappalardo, G., Amodeo, A., Apituley, A., Comeron, A., Freudenthaler, V., Linné, H., Ansmann, A., Bösenberg, J.,
10   D'Amico, G., Mattis, I., Mona, L., Wandinger, U., Amiridis, V., Alados-Arboledas, L., Nicolae, D., and Wiegner, M.: EARLINET: towards an advanced sustainable European aerosol lidar network, Atmos. Meas. Tech., 7, 2389-2409, doi:10.5194/amt-7-2389-2014, 2014.

Pérez-Ramírez, D., Lyamani, H., Olmo, F. J., Whiteman, D. N., and Alados-Arboledas, L.: Columnar aerosol properties from sun and- star photometry: statistical comparisons and day-to-night dynamic, Atmos. Chem. Phys., 12, 9719–9738,
15   doi:10.5194/acp- 12-9719-2012, 2012.

Pérez-Ramírez, D., Veselovskii, I., Whiteman, D. N., Suvorina, A., Korenskiy, M., Kolgotin, A., Holben, B., Dubovik, O., Siniuk, A., and Alados-Arboledas, L.: High temporal resolution estimates of columnar aerosol microphysical parameters from spectrum of aerosol optical depth by linear estimation: application to long-term AERONET and star-photometry measurements, Atmos. Meas. Tech., 8, 3117-3133, doi:10.5194/amt-8-3117-2015, 2015.

20   Pérez-Ramírez, D., Lyamani, H., Smirnov, A., O'Neill, N.T., Veselovskii, I., Whiteman, D.N., Olmo, F.J., Alados-Arboledas, L.: Statistical study of day and night hourly patterns of columnar aerosol properties using sun and star photometry. Proceedings of SPIE – The International Society for Optical Engineering, 100001, Article Number 100010K, 2016.

Perrone, M. R., De Tomasi, F., and Gobbi, G. P.: Vertically resolved aerosol properties by multi-wavelength lidar
25   measurements, Atmos. Chem. Phys., 14, 1185-1204, doi:10.5194/acp-14-1185-2014, 2014.

Preißler, J., Wagner, F., Pereira, S. N., and Guerrero-Rascado, J. L.: Multiinstrumental observation of an exceptionally strong Saharan dust outbreak over Portugal, J. Geophys. Res., 116, D24204, doi:10.1029/2011JD016527, 2011.

Rolph, G.D.: Real-time Environmental Applications and Display sYstem (READY) Website (http://www.ready.noaa.gov). NOAA Air Resources Laboratory, College Park, MD, 2016.

30   Román, R., Torres, B., Fuertes, D., Cachorro, V. E., Dubovik, O., Toledano, C., Cazorla, A., Barreto, A., Bosch, J.L., Lapyonok, T., González, R., Goloub, P., Perrone, M.R., Olmo, F.J., de Frutos, A., Alados-Arboledas, L.: Remote sensing of lunar aureole with a sky camera: Adding information in the nocturnal retrieval of aerosol properties with GRASP code, Remote Sens. Environ., 196, 238-252, doi:10.1016/j.rse.2017.05.013, 2017.

Schuster, G. L., Dubovik, O., and Arola, A.: Remote sensing of soot carbon – Part 1: Distinguishing different absorbing aerosol species, Atmos. Chem. Phys., 16, 1565-1585, doi:10.5194/acp-16-1565-2016, 2016.

Shipley, S. T., Tracy, D. H., Eloranta, E. W., Trauger, J. T., Sroga, J. T., Roesler, F. L., and Weinman, J. A.: High Spectral ResolutionLidar to Measure Optical-Scattering Properties of Atmospheric Aerosols, 1. Theory and Instrumentation, Appl. Optics, 22, 3716–3724, doi:10.1364/AO.22.003716, 1983.

Stein, A.F., Draxler, R.R, Rolph, G.D., Stunder, B.J.B., Cohen, M.D., and Ngan, F.: NOAA's HYSPLIT atmospheric transport and dispersion modeling system, Bull. Amer. Meteor. Soc., 96, 2059-2077, 2015.

Titos, G., del Águila, A., Cazorla, A., Lyamani, H., Casquero-Vera, J.A., Colombi, C., Cuccia, E., Gianelle, V., Močnik, G., Alastuey, A., Olmo, F.J., Alados-Arboledas L.: Spatial and temporal variability of carbonaceous aerosols: Assessing the impact of biomass burning in the urban environment, Science of The Total Environment, Volume 578, doi:10.1016/j.scitotenv.2016.11.007, 2017.

Toledano, C., Wiegner, M., Groß, S., Freudenthaler, V., Gasteiger, J., Müller, D., Müller, T., Schladitz, A., Weinzierl, B., Torres, B., and O'neill, N. T.: Optical properties of aerosol mixtures derived from sun-sky radiometry during SAMUM-2, Tellus B, 63, 635–648, doi:10.1111/j.1600-0889.2011.00573.x, 2011.

Torres, B., Dubovik, O., Toledano, C., Berjon, A., Cachorro, V. E., Lapyonok, T., Litvinov, P., and Goloub, P.: Sensitivity of aerosol retrieval to geometrical configuration of ground-based sun/sky radiometer observations, Atmos. Chem. Phys., 14, 847-875, doi:10.5194/acp-14-847-2014, 2014.

Torres, B., Dubovik, O., Fuertes, D., Schuster, G., Cachorro, V. E., Lapionak, T., Goloub, P., Blarel, L., Barreto, A., Mallet, M., Toledano, C., and Tanré, D.: Advanced characterization of aerosol properties from measurements of spectral optical depth using the GRASP algorithm, Atmos. Meas. Tech., Accepted., 2017.

Valenzuela, A., Olmo, F. J., Lyamani, H., Antón, M., Quirantes, A., and Alados-Arboledas, L.: Classification of aerosol radiative properties during African desert dust intrusions over southeastern Spain by sector origins and cluster analysis, J. Geophys. Res., 117, D06214, doi:10.1029/2011JD016885, 2012a.

Valenzuela, A., Olmo, F. J., Lyamani, H., Antón, M., Quirantes, A., and Alados-Arboledas, L.: Analysis of the desert dust radiative properties over Granada using principal plane sky radiances and spheroids retrieval procedure, Atmos. Res., 104–105, 292–301, doi:10.1016/j.atmosres.2011.11.005, 2012b.

Veselovskii, I., Kolgotin, A., Griaznov, V., Müller, D., Wandinger, U., and Whiteman, D. N.: Inversion with regularization for the retrieval of tropospheric aerosol parameters from multiwavelength lidar sounding, Appl. Opt., 41, 3685–3699, doi:10.1364/AO.41.003685, 2002.

Wandinger, U. and Ansmann, A.: Experimental Determination of the Lidar Overlap Profile with Raman Lidar, Appl. Opt., 41, 511– 514, doi:10.1364/AO.41.000511, 2002.

Whiteman, D. N., Melfi, S. H., and Ferrare, R. A.: Raman lidar system for the measurement of water vapor and aerosols in the Earth's atmosphere, Appl. Optics, 31, 3068–3082, doi:10.1364/AO.31.003068, 1992.

Whiteman, D.N., Pérez-Ramírez, D., Veselovskii, I., Colarco, P., Buchard, V.: Simulations of spaceborne multiwavelength lidar measurements and retrievals of aerosol microphysics. Journal of Quantitative Spectroscopy and Radiative Transfer, acepted, 2017.

Wiedensohler, A., Birmili, W., Nowak, A., Sonntag, A., Weinhold,K., Merkel, M., Wehner, B., Tuch, T., Pfeifer, S., Fiebig, M.,Fjäraa, A. M., Asmi, E., Sellegri, K., Depuy, R., Venzac, H., Villani,P., Laj, P., Aalto, P., Ogren, J. A., Swietlicki, E., Williams,P., Roldin, P., Quincey, P., Hüglin, C., Fierz-Schmidhauser, R.,Gysel, M., Weingartner, E., Riccobono, F., Santos, S., Grüning,C., Faloon, K., Beddows, D., Harrison, R., Monahan, C., Jennings,S. G., O'Dowd, C. D., Marinoni, A., Horn, H.-G., Keck,L., Jiang, J., Scheckman, J., McMurry, P. H., Deng, Z., Zhao, C.S., Moerman, M., Henzing, B., de Leeuw, G., Löschau, G., andBastian, S.: Mobility particle size spectrometers: harmonization of technical standards and data structure to facilitate high quality long-term observations of atmospheric particle number sized distributions, Atmos. Meas. Tech., 5, 657–685, doi:10.5194/amt-5-657-2012, 2012.

5

10

Tables

Table 1. Instruments on board the ATR-42 aircraft during F30 and F31 flights.

Parameter measured	Instrument	Abbreviation	Scientific objective	Nominal size range (µm)	Wavelength (nm)
Size distribution	Forward Scattering Spectrometer Probe, Model 300, Particle Measuring Systems	FSSP-300	Coarse mode conc.	0.28 – 20	632.8
	Sky-Optical Particle Counter, model 1.129, Grimm Technik	GRIMM	Coarse mode conc.	0.25 – 32	655
	Ultra-High Sensitivity Aerosol Spectrometer Droplet Measurement Technologies	UHSAS	Aiken + accumulation mode conc.	0.04 – 1	1054
	Scanning mobility particle sizer, custom-built	SMPS	Aiken + accumulation mode conc.	0.03 – 0.4	n/a
Optical properties	3λ Integrated Nephelometer, Model 3563, TSI	Nephelometer	Scattering coefficient	n/a*	450, 550, 700
	Cavity Attenuated Phase Shift, Aerodyne Research Inc.	CAPS	Extinction coefficient	n/a*	530
	Photomètre Léger Aéroporté pour la Surveillance des Masses d'Air	PLASMA	Extinction coefficient, AOD	n/a*	340-2250

*not applicable

Table 2. Input and output information used for LIRIC and GRASP retrievals.

	LIRIC		GRASP	
	<u>SUN-PHOTOMETER*</u> • AOD • VC • RRI and IRI • % Sphericity	<u>LIDAR</u> Elastic backscattered signal: • 355, 532 and 1064 nm • 532-cross polarized signal	<u>SUN-PHOTOMETER</u> • AOT or AOD • Total scattered radiances At 440, 670, 870 and 1020 nm	<u>LIDAR</u> Elastic backscattered signal: • 355, 532 and 1064 nm
INPUT				
OUTPUT	• VC profile for fine and coarse mode		<u>Columnar (fine and coarse)</u> • SD • RRI and IRI • VC • r$_{eff}$ • SSA • LR • % Sphericity (total)	<u>Vertical (fine and coarse)</u> • VC • α and β • SSA

*AERONET product

Table 3. Columnar effective radius and particle volume concentration for coarse and fine particles modes retrieved by GRASP and AERONET algorithms.

			16th June 2013		17th June 2013	
			Granada	Cerro Poyos	Granada	Cerro Poyos
Effective radius (µm)	GRASP	fine	0.12	0.13	0.10	0.12
		coarse	2.2	2.2	2.4	2.2
	AERONET	fine	0.12	0.11	0.11	0.12
		coarse	1.9	1.9	2.1	1.9
Volume concentration (µm³/µm²)	GRASP	fine	0.018	0.017	0.018	0.011
		coarse	0.17	0.15	0.14	0.13
	AERONET	fine	0.015	0.015	0.016	0.010
		coarse	0.14	0.13	0.12	0.11

**Table 4.** Comparison of fine, coarse and total mean volume concentration (µm³/cm³) retrieved by GRASP, measured by airborne and retrieved by LIRIC for dust layers on 16th (up to 4.5 km a.s.l.) and 17th (from 2.6 to 5.0 km a.s.l.) June.

Volume concentration ($\mu m^3/\mu m^2$)		16th June 2013		17th June 2013	
		Granada	Cerro Poyos	Granada	Cerro Poyos
Fine	GRASP	4.7 ±0.6	5.5 ±0.3	5.5 ±1.3	3.5 ±1.0
	AIRBORNE	2.6 ±0.4	2.6 ±0.4	1.9 ±0.6	1.9 ±0.6
	LIRIC	4.2 ±0.8	4.6 ±1.0	5.3 ±1.3	2.8 ±1.1
Coarse	GRASP	28 ±4	32 ±4	35 ±7	36 ±5
	AIRBORNE	31 ±8	27 ±5	41 ±11	41 ±11
	LIRIC	37 ±4	46 ±4	35 ±5	38 ±6
Total	GRASP	33 ±4	38 ±4	40 ±8	39 ±6
	AIRBORNE	33 ±8	28 ±5	42 ±11	42 ±11
	LIRIC	41 ±5	50 ±4	40 ±6	41 ±6

Table 5. Mean value of backscatter - Angström exponent (β-AE) and Color Ratio (CR) between 532 and 1064 nm, retrieved by GRASP for dust layers on 16th and 17th June 2013.

	16th June 2013		17th June 2013	
	Granada	Granada	Granada	Granada
β-AE	0.65 ±0.07	0.46 ±0.05	0.63 ±0.12	0.40 ±0.10
CR	1.15 ±0.05	1.13 ±0.05	1.09 ±0.09	1.08 ±0.04

Figures
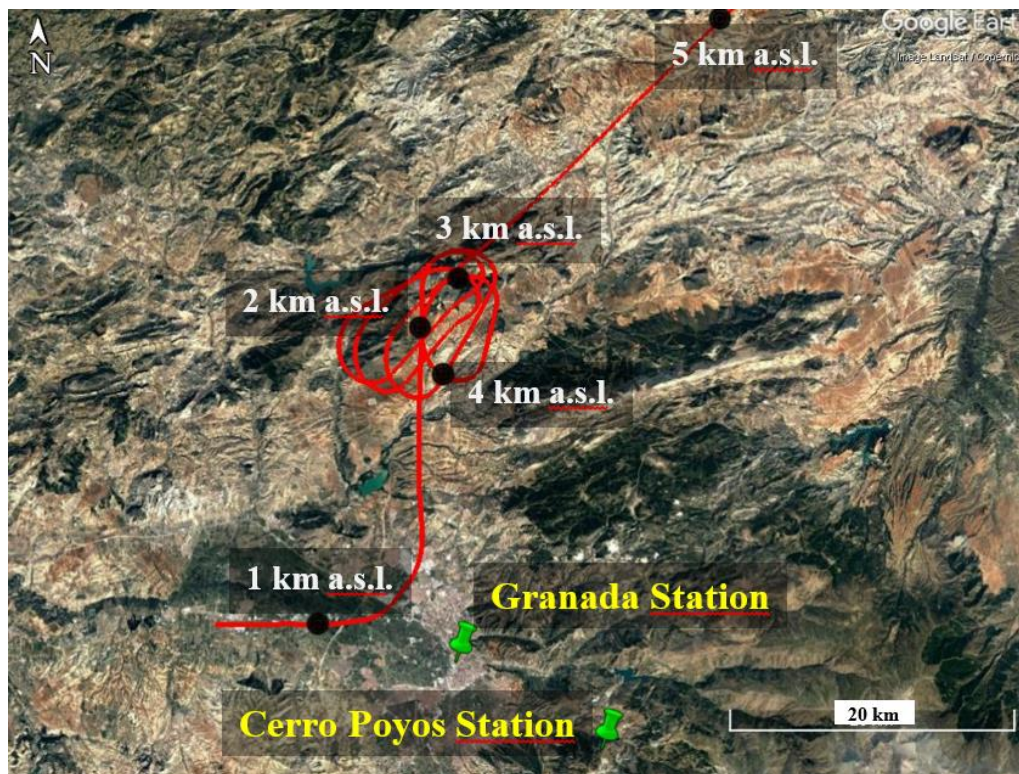
Figure 3. Map illustrating the Granada and Cerro Poyos stations. The red line indicates the trajectory and the black points the altitude of the aircraft on 17th June.
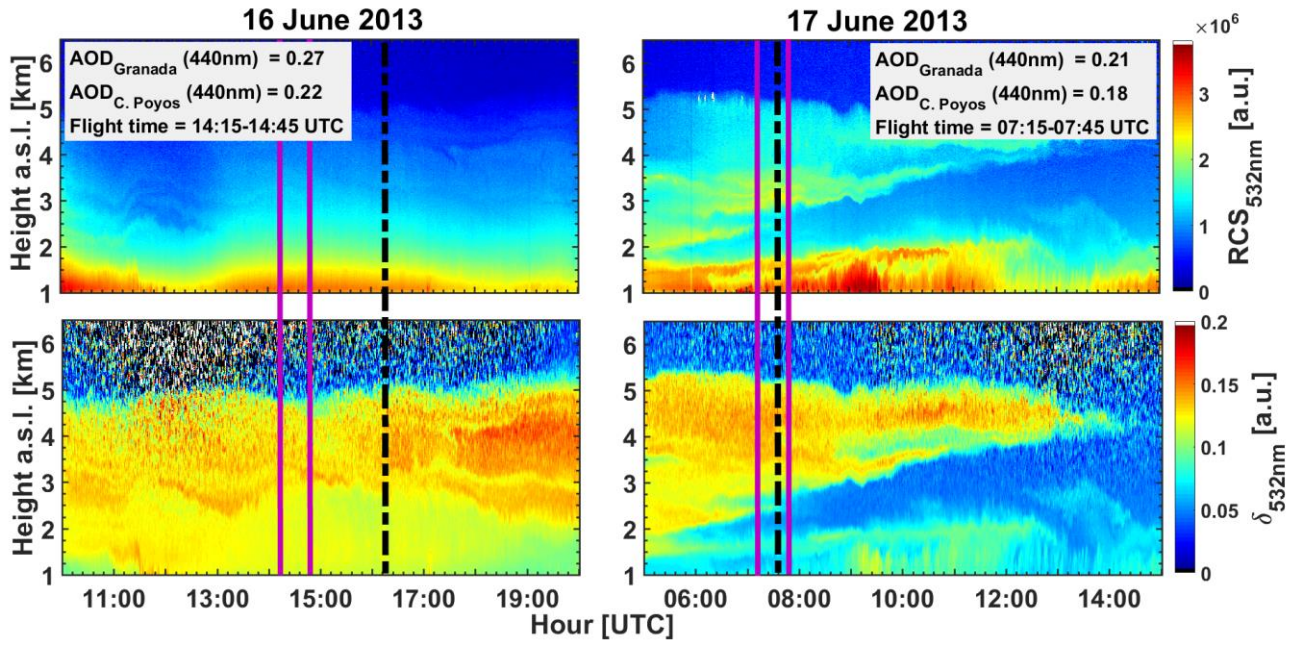
Figure 4. Temporal evolution of the lidar range corrected signal (top) and the depolarization ratio (bottom) at 532nm on 16th (left) and 17th (right) June, 2013. The two purple lines indicate the lidar analyzed interval. The black dashed line indicates the sun-photometer measurements.
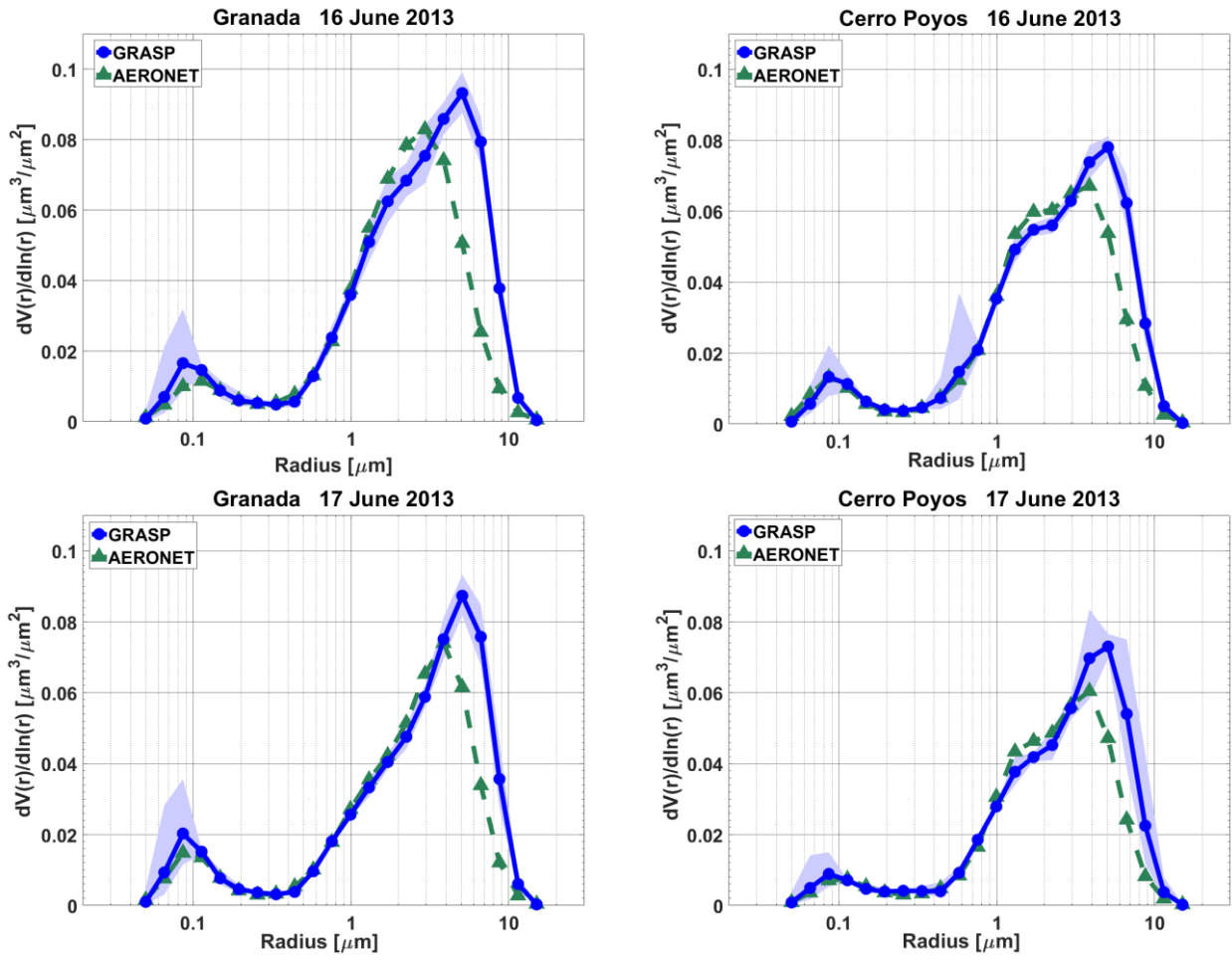
5

10

15

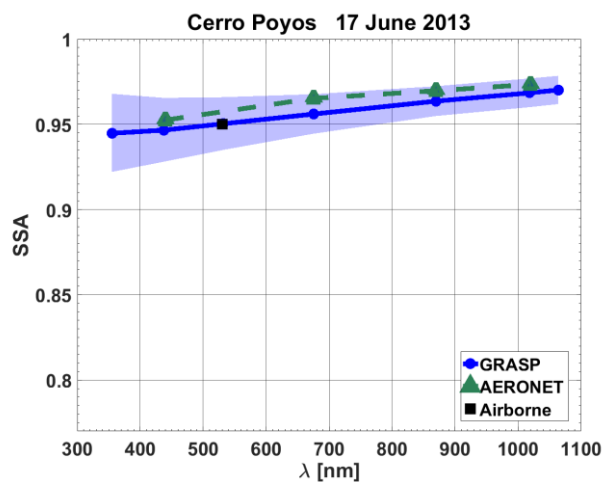**Figure 5.** Size distribution retrieved by GRASP (blue) with its uncertainty (shaded area) and by AERONET (green) on 16th (top) and 17th (bottom) June 2013 at Granada (left) and Cerro Poyos (right).

5
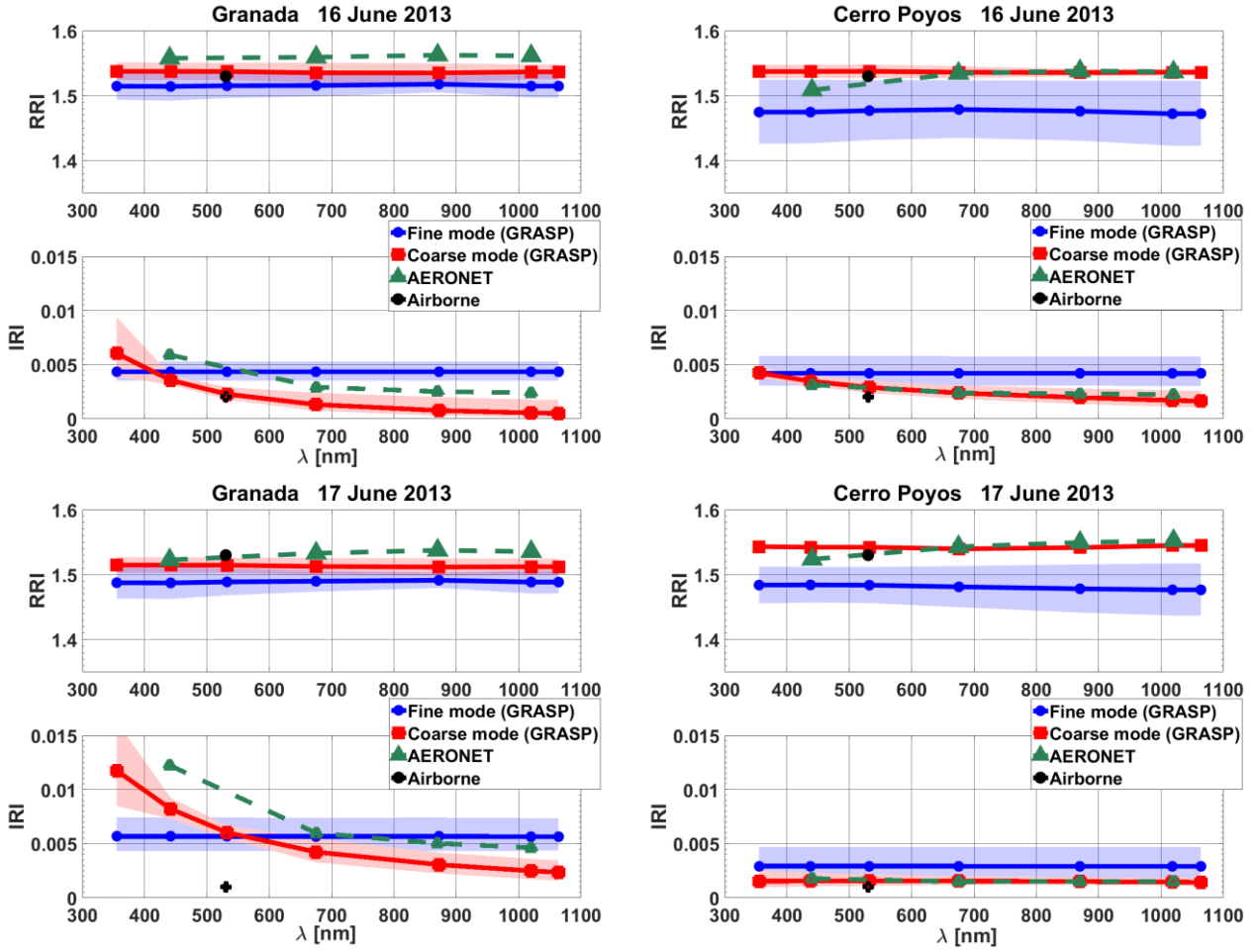
Figure 4. Spectral real (RRI) and imaginary (IRI) refractive indices retrieved by GRASP for the fine (blue) and coarse (red) modes with its uncertainty (shaded area); by AERONET (green) and airborne measurement (black) on 16th (top) and 17th (bottom) June 2013 in Granada (left) and Cerro Poyos (right).
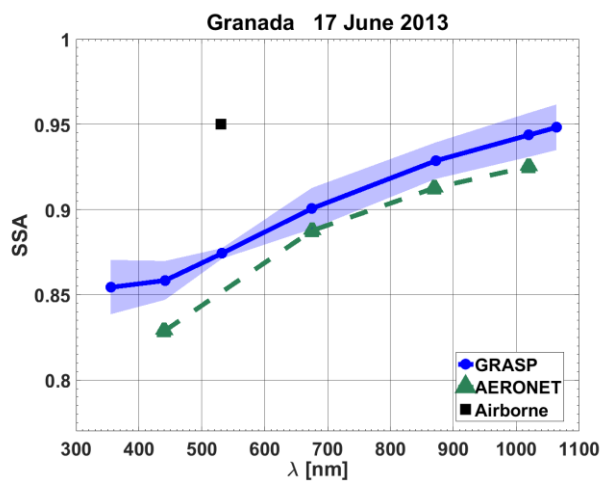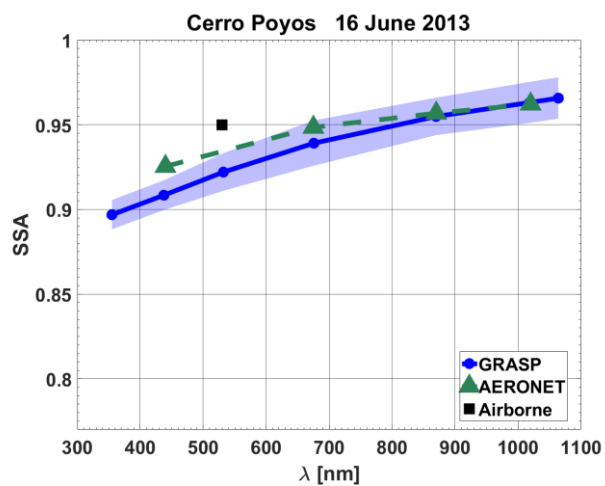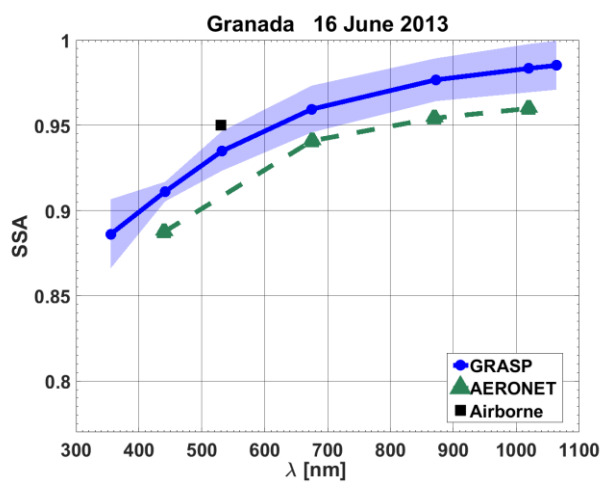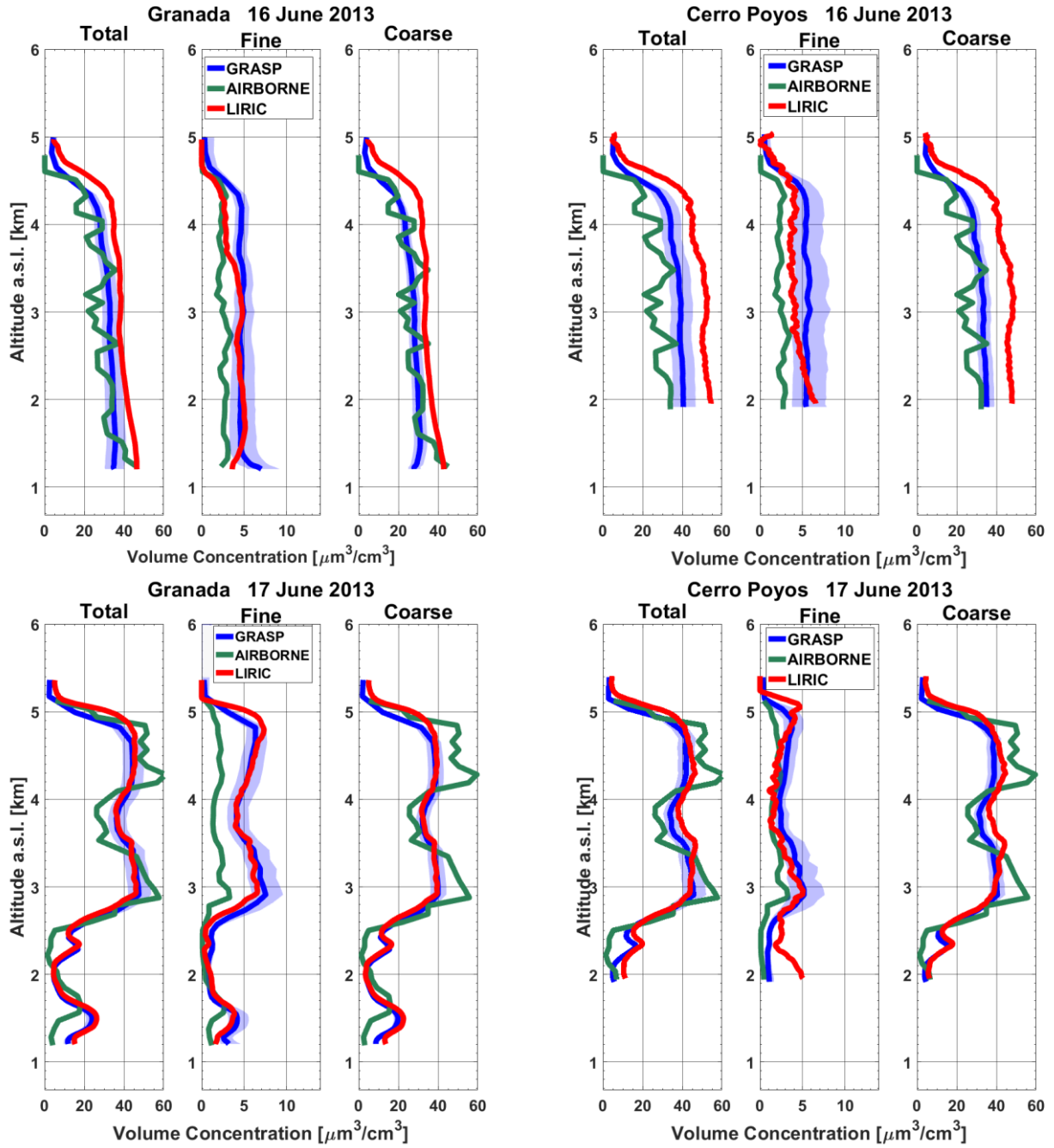
Figure 5. Single-scattering albedo retrieved by GRASP (blue) with its uncertainty (shaded area), AERONET (green) and airborne measurement (black) on 16th (top) and 17th (bottom) June 2013 at Granada (left) and Cerro Poyos (right).

5

10

15

Figure 6. Volume concentration profile (total, fine and coarse mode) retrieved by GRASP (blue) with its uncertainty (shaded area), aircraft measurements (green) and LIRIC (red) on 16th (top) and 17th (bottom) June 2013 at Granada (left) and Cerro Poyos (right).

5
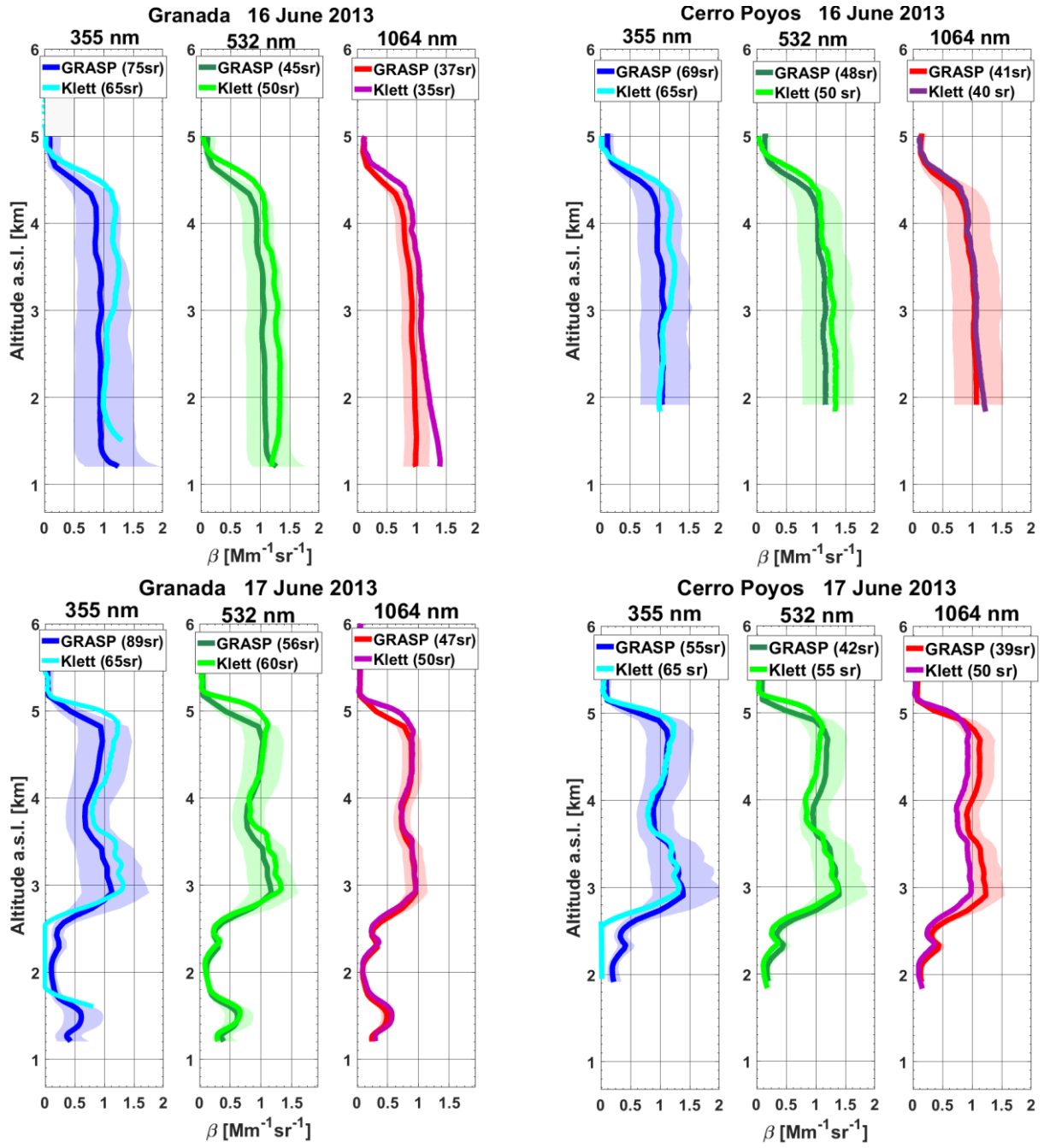
Figure 7. Aerosol backscatter coefficient profiles retrieved at 355, 532 and 1064 nm by GRASP with its uncertainty (shaded area) and Klett-Fernald on 16th (up) and 17th (down) June 2013 at Granada (left) and Cerro Poyos (right).
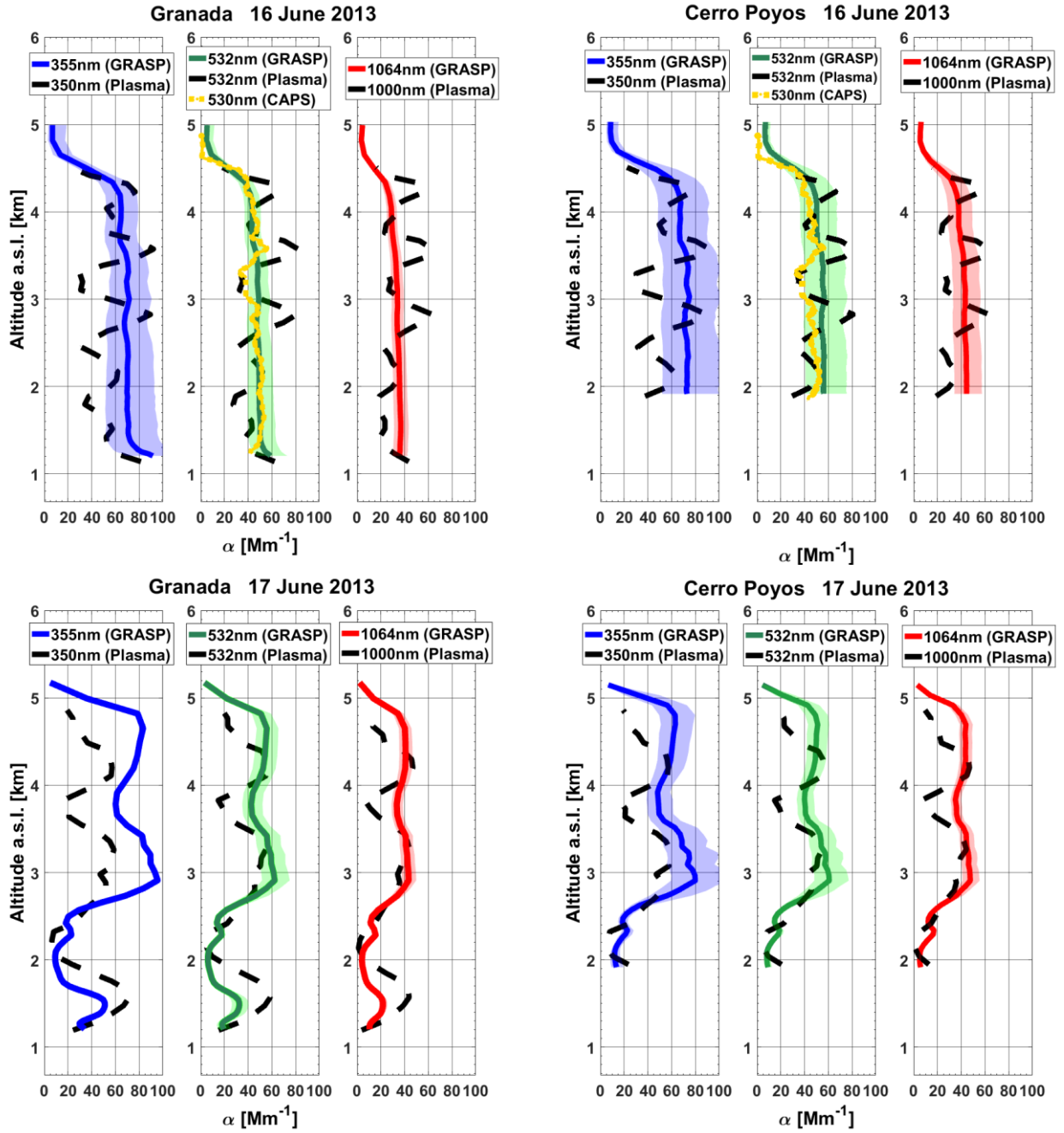
5

Figure 8. Aerosol extinction coefficient profiles retrieved by GRASP (355, 532 and 1064 nm) with its uncertainty (shaded area), PLASMA (350, 530 and 1000 nm) and CAPS (530 nm) on 16th (top) and 17th (bottom) June 2013 at Granada (left) and Cerro Poyos (right).
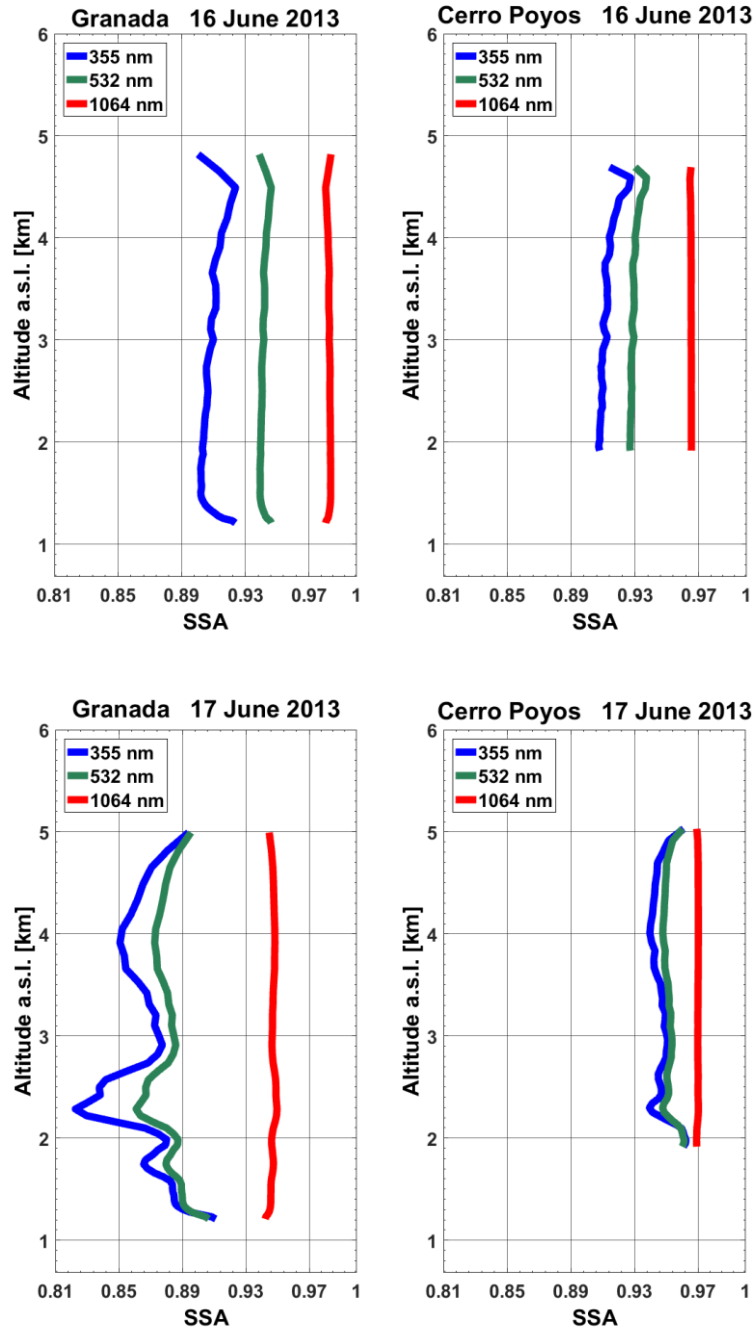
Figure 9. Single scattering albedo profiles at 355, 532 and 1064 nm retrieved by GRASP on 16th (up) and 17th (down) June 2013 at Granada (left) and Cerro Poyos (right).
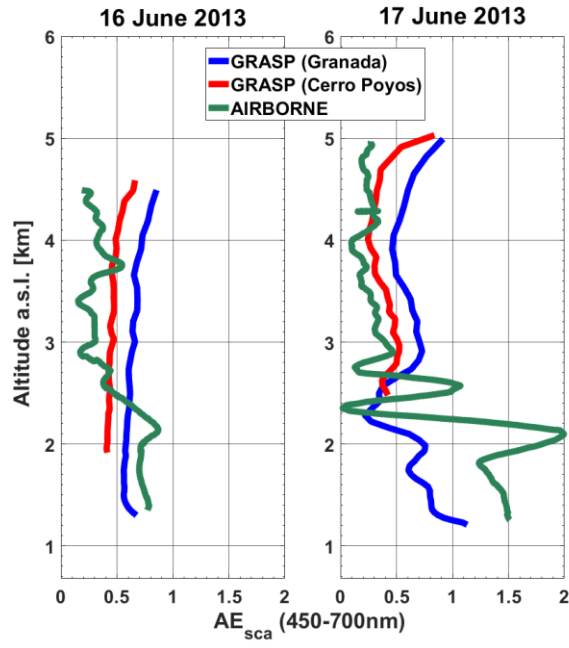
5

Figure 10. Scattering – Angström Exponent (450 - 700 nm) retrieved by GRASP (blue and red) at Granada and Cerro Poyos, respectively, and aircraft measurements (green) on 16th (left) and 17th (right) June 2013.

5